Functional characterization of MIMP for its adhesion to the intestinal epithelium

Zhihua Liu[1], Tongyi Shen[2], Hongqi Chen[1], Yukun Zhou[1], Peng Zhang[1], Yanlei Ma[1], Mary Pat Moyer[3], Ming Zhang[1], Zhaoxin Chu[1], Huanlong Qin[1]

[1]Department of Surgery, Shanghai Jiao Tong University Affiliated Sixth People's Hospital, Shanghai, 200233, China, [2]Department of Surgery, Shanghai, 200072, Shanghai Tenth People's Hospital, China, [3]INCELL Corporation, San Antonio Texas, 78249, United States of America

TABLE OF CONTENTS

1. ABSTRACT

The micro integral membrane protein (MIMP), the domain within the integral membrane protein of *Lactobacillus plantarum* CGMCC 1258, has been shown to adhere to mucin and antagonize the adhesion of enteroinvasive *E. coli* and enteropathogenic *E. coli*. To further characterize the functions of MIMP, we investigated its effects on the intestinal permeability, expression of tight junction (TJ) proteins and TJ ultrastructure *in vitro* and *in vivo*. We also determined the interaction between MIMP and dendritic cells (DCs). We observed that MIMP reduced intestinal permeability and restored the expression and distribution of TJ proteins in both NCM460 cell monolayers and in IL-10$^{-/-}$ mice. MIMP adhered to immature (i) DCs by binding to DC-SIGN, and induced DCs to produce anti-inflammatory cytokines and to mediate Th2 differentiation. Moreover, MIMP stimulated the expression of anti-inflammatory cytokines in colonic mucosa and attenuated colitis in IL-10$^{-/-}$ mice. In conclusion, MIMP is the main functional component of *L. plantarum* that contributes to its protective effects, and thus may be a potential therapeutic agent for intestinal diseases.

2. INTRODUCTION

The bacteria of the genus *Lactobacilli* that reside in the mammalian gut play an important role in maintaining the homeostasis of gut flora (1-2). Dysbiosis exists in patents with inflammatory bowel disease (IBD), which manifests as ulcerative colitis (UC) and Crohn's disease (CD) and is characterized by increased bacteroides, adherent/invasive *E. coli*, enterococci, and *Clostridum perfrigens*, and reduced bifidobacterium and lactobacillus species (3-5). Over the past decades, treatment with probiotics, including lactic acid bacteria, has been proven to be effective in patients with colonic inflammation (6-8). However, the precise molecular mechanisms of action of probiotics have not been fully elucidated; there is, however, evidence indicating that the modulation of the gut flora itself, improvement of the intestinal epithelial barrier function, and direct effects on the epithelial and immune cells may all contribute (9).

It has been established that adhesion of Lactobacilli to the epithelium is a key process regulating the functional interactions between Lactobacilli and the intestinal tract of the host (10). Adhesion is initiated from non-specific physical interactions between the two surfaces, followed by the activation of the specific adhesion between special ligands of the bacteria and their corresponding receptors on the intestinal cells (10-11). These ligands are adhesins that are located on the surface layer of the bacteria or secreted from the bacteria, and mediate the adhesion of bacteria to the target cells of the intestinal tract and subsequently activate the signal transduction pathways that modulate gut-barrier function and local systemic inflammatory responses (12-13). Furthermore, the adhesins competitively block the adhesion of other pathogenic bacteria to the proximal intestinal epithelium (13-14).

The surface layer proteins (SLPs) of Lactobacilli, which are important components of the cell envelope structures, have been shown to be critical for proper adhesion of Lactobacilli to the intestinal epithelium (13-16). It is known that some structural regions of the SLPs are responsible for the adhesion of the bacteria to the intestinal epithelium. However, due to the unique hydrophilic and hydrophobic property, purification of SLPs is technically difficult, and consequently, only a few studies have explored the role of SLPs (14, 16-17).

It has also demonstrated that *Lactobacilli* exert their probiotic properties by regulating immune system functions through dendritic cells (DCs) (18-19). As professional antigen-presenting cells, DCs have been identified in numerous tissue compartments, including the lamina propria, the subepithelium, a T cell-rich zone of lymphoid tissue associated with the mucosa, and draining lymph nodes (20). Precursors of immature DCs (iDCs) that migrate through the bloodstream are recruited by chemokines released by gut epithelial cells, and reach the epithelial cells expressing occludin and claudin-1 molecules, which facilitate these cells capability to penetrate into the tight junction (TJ) between epithelial cells and settle in or beneath the epithelium as iDCs or mature DCs (21). Subsequently, DCs in the epithelium extend their probing dendrites into the lumen to sample commensal or microbial immunogens (22-25). Meanwhile, DCs located in or beneath the epithelium play an essential role in sampling and capturing various bacterial antigens that cross the epithelial layer (26-27), bridging the innate and adaptive immune processes and initiating the appropriate immune responses (28-29). Based on the microbial stimulus encountered, DCs may enhance the differentiation of unprimed, naive T cells toward Th1, Th2, unpolarized T cells, or T regulatory cell responses (30). DCs can migrate into the lymphoid follicles, wherein processed antigens are presented to B or T cells to initiate humoral (IgA) or cellular immune responses (31). Previous study showed that C-type lectin receptor (CLR), DC-SIGN played an important role in the interaction of lactobacillus/SLP and DCs, while the antibody of DC-SIGN, AZN-D1, or the Ca^{2+} chelator EDTA may block this interaction (18).

NCM460, a cell line derived from normal human colon mucosal epithelium, has been applied exclusively in various intestinal research areas, especially infectious disease (32-34). As a normal human colon cell line, NCM460 expresses colonic epithelial cell-associated antigens, such as cytokeratins and villin.

Interleukin-10 knock-out (IL-10$^{-/-}$) mice are a well-established model of chronic enterocolitis (35-36), and the development of intestinal inflammation is associated with a defect in the epithelial barrier integrity that allows sufficient passage of bacteria or bacterial antigens to initiate a mucosal immune response, leading to increased intestinal permeability and epithelial barrier dysfunction (37). In IL-10$^{-/-}$ mice, lymphocyte development and antibody responses are normal, but most animals are growth-retarded, anemic, and suffer from chronic

enterocolitis (38). Recently, this model has been used for the investigation of the efficacy of probiotics and their active ingredients in attenuating intestinal injury (39-41).

Lactobacillus plantarum, one of Lactobacilli, has been shown to be effective in the treatment and prevention of colitis in mice (42-43). Indeed, our recent *in vitro* and *in vivo* studies have also indicated that *L. plantarum* exerts its therapeutic effects by adhering to the epithelial cells, restoring the tight junction structure and function, and improving paracellular permeability (44-47). In our previous study (detailed in our simultaneously submitted manuscript) of the SLP integrated membrane protein (IMP) from *L. plantarum* strain CGMCC 1258, we identified a peptide, namely IMP-2, that is responsible for the adhesion property of the strain. Moreover, the smallest active domain within IMP-2, named micro IMP (MIMP), was successfully identified and purified, and its adhesion activity was verified in a normal human colon mucosal epithelial cell line, NCM460.

Therefore, the aim of the present study was to further functionally characterize MIMP by determining its effects on the intestinal barrier function and immune responses. In the present study, the protective effects of MIMP on epithelial barrier dysfunction of NCM460 cells, as caused by enteroinvasive *Escherichia coli* (EIEC) and enteropathogenic *E. coli* (EPEC), was determined. The interactions between MIMP and DCs, which have been reported to play a critical role in the regulation of immune system functions induced by Lactobacilli (18-19), and the subsequent DC-driven Th1/Th2 differentiation were investigated. Moreover, IL-10$^{-/-}$ mice were used to determine the *in vivo* effects of MIMP on epithelial paracellular permeability, histological changes and the epithelial barrier function.

3. MATERIALS AND METHODS

3.1. MIMP, antibodies and major reagents

Recombinant MIMP was expressed from *E. coli* as described in our previous study (our simultaneously submitted manuscript). Primary antibodies including those against TJ proteins (i.e. claudin-1, occludin, JAM-1, and ZO-1), F-actin (a cell cytoskeleton element), IFN-γ–fluorescein isothiocyanate (FITC) and IL-4–phycoerythrin and costimulatory molecules, CD80, CD86 and MHC-II, were purchased from Abcam (MA, USA). Secondary antibodies, including FITC-conjugated specific antibody, horse radish peroxidase (HRP)-conjugated anti-rabbit IgG, and HRP-conjugated anti-human IgG antibodies, were purchased from Sigma (MO, USA). AZN-D1, a neutralizing antibody against the DC-specific ICAM-3-grabbing nonintegrin (DC-SIGN), one of the specific CLRs, was from Beckman Coulter (Roissy, France). Polyclonal antibodies against MIMP were generated as described in the simultaneously submitted manuscript.

Ethylenediaminetetraacetic acid (EDTA) solution, D-mannose, brefeldin A and saponin were from Sigma-Aldrich (Steinheim, Germany). De Man-Rogosa-Sharpe (MRS) broth was from Difco Laboratories (MI,

USA). Dulbecco's modified Eagle's medium (DMEM), Iscove's Modified Dulbecco's Medium, fetal bovine serum (FBS) and trizol reagent were from GIBCO (CA, USA). Penicillin and streptomycin were from Invitrogen Corp. (CA, USA). AT-1001, a zonulin receptor antagonist, was purchased from Alba Therapeutics (MD, USA). Recombinant interleukin-2 (IL-2), IL-4, human granulocyte/macrophage colony-stimulating factor (GM-CSF), paraffin oil, lactulose, mannitol, sucralose, phenyl-β-D-thiogalactoside, prostaglandin E2 (PGE$_2$), bovine serum albumin (BSA), phosphate buffered saline (PBS) and *E. coli* lipopolysaccharide (LPS) were purchased from Sigma. FITC labeling kits, enzyme-linked immunosorbent assays (ELISA) kits and FITC conjugated DC-SIGN (DC-SIGN-Fc) were purchased from Cell Sciences (MA, USA). Alexa Fluor 647 dextran (10 kDa) and 4-(4-(Didecylamino)styryl)-N-methylpyridinium iodide (4-Di-10-ASP, or DiA) was purchased from Molecular Probes Inc. (OR, USA).

3.2. Bacterial strains and culture conditions

L. plantarum CGMCC 1258 (generously provided by Dr. Xiaomin Hang, the Institute of Bio-medicine, Shanghai Jiao Da Onlly Company Ltd, Shanghai, China) was inoculated in 5% fresh MRS broth at 37°C for 24 h, harvested by centrifugation (×3500g) at 4°C for 20 min, and washed with 50 mL 0.01M PBS (pH 7.4). The EIEC strain ATCC 43893 (O124:NM) and EPEC strain ATCC 43887 (O111:NM) (both from Shanghai Municipal Center for Disease Control and Prevention, Shanghai, China) were grown in static DMEM at 37°C for 24 h. Quantification of bacterial density was measured at 600 nm (Beckman DU-50 spectrophotometer) with the colony forming units (cfu).

3.3. NCM460 cells, iDCs and mice

NCM460 cells were purchased from INCELL Corporation (San Antonio, TX, USA) and cultured in M3 media supplemented with 10% FBS, 100 U/ml penicillin and 100 μg/ml streptomycin at 37°C in a 95% humidified atmosphere with 5% CO2, as previously described (32).

iDCs were obtained from the buffy coats of healthy donors, as described elsewhere (48). Briefly, human peripheral blood mononuclear cells were isolated by a Ficoll gradient. Monocytes were isolated by CD14 magnetic microbeads (MACS; Miltenyi Biotec, CA, USA) and differentiated into iDCs in the presence of IL-4 and human GM-CSF (500 and 800 U/mL, respectively). Then, iDCs were sub-cultured in Iscove's Modified Dulbecco's Medium, supplemented with 10% FBS, 500 U/mL IL-4, and 800 U/mL GM-CSF.

Homozygous IL-10$^{-/-}$ mice were generated on a wild-type 129 Sv/Ev genetic background, bred and raised in the animal facility at Shanghai Jiao Tong University School of Medicine; they were housed under specific pathogen-free conditions until weaning (3 weeks) when they were moved to a conventional animal unit. The mice were housed in cages with a high-efficiency particulate air filter and fed with a standard mouse chow diet. IL-10$^{-/-}$ mice at age of 3.5 weeks were randomized into five groups

Table 1. Experimental grouping of NCM460 cells

Group	Description
Control	Cell monolayers with no infection and no treatment
EIEC or EPEC	Cell monolayers infected by EIEC or EPEC
L. plantarum +EIEC or EPEC	Cell monolayers infected by EIEC or EPEC and treated with L. plantarum
MIMP +EIEC or EPEC	Cell monolayers infected by EIEC or EPEC and treated with MIMP
Anti-MIMP+MIMP +EIEC or EPEC	Cell monolayers pre-incubated for 2 h with polyclonal anti-MIMP antibodies, then infected with EIEC or EPEC and treated with MIMP

EIEC, enteroinvasive *E. coli*; EPEC, enteropathogenic *E. coli*; MIMP, micro integral membrane protein. wo parallel experiments were carried out separately for EIEC and EPEC.

(=10 for each group), and were treated with oral gavage of milk alone or containing 1×10^9 cfu/mL *L. plantarum*, MIMP (0.1 μg/mL), or AT-1001 (10 mg/mL), respectively. Wild-type mice at age of 3.5 weeks were treated with oral gavage of either milk or milk containing 0.1 μg/mL MIMP (n=10 for each group). The volume of gavage was 0.5 mL. Mice were treated up to the age of 17 weeks when they were sacrificed by cervical dislocation. The experimental protocol was approved by the Animal Care and Use Committee and the Ethics Committee of Shanghai Jiao Tong University.

3.4. Determination of MIMP effect on the intestinal permeability *in vitro*, *ex vivo* and *in vivo*
3.4.1. Measurement of transepithelial electrical resistance (TER) in NCM460 cell monolayers
        NCM460 cells were grown on filters (Millicell culture plate inserts; 0.4 μm pore size; 0.6 cm2) at 37°C in a 95% humidified atmosphere, with 5% CO_2. At full confluence (10-14 days) (i.e. a monolayer was formed), a TER of >450 Ωcm2 was achieved as measured by using a voltmeter (Millicell-ERS; Millipore, MA, USA). The intestinal epithelial monolayers were treated with EIEC or EPEC in the presence or absence of *L. plantarum* or MIMP with or without 2-h pre-treatment of polyclonal anti-MIMP antibodies, as described as Table 1. In infection groups, 100 μL EIEC ATCC43893 (O124:NM) and EPEC ATCC43887 (O111:NM) at 1.0×10^8/mL were, respectively, added to the apical side of the cell culture insert for rapid infection of the monolayer, with an inoculation ratio of EIEC/EPEC to NCM460 cells of 100:1, and the insert was placed in a 50-mL tube and centrifuged at ×200 g for 4 min. In *L. plantarum* and MIMP groups, *L. plantarum* (100 μL of 1.0×10^8/mL) and MIMP (100 μL of 0.1 ng/mL) purified from the whole cell proteins of transfected *E. coli* were, respectively, added onto the monolayer of NCM460 cells simultaneously with the EIEC/EPEC infection. In antibody groups, NCM460 cells were pre-incubated with the serum containing polyclonal antibodies against MIMP (100 μL of dilution 1:5000) prepared as described above, prior to infection with EIEC or EPEC which were simultaneously incubated with *L. plantarum* or MIMP. NCM460 cells cultured under the same conditions but without pre-incubation with the serum, infection of EIEC/EPEC, and addition of *L. plantarum* or MIMP served as the control group. Two experiments were performed separately for EIEC and EPEC.

        The integrity of the confluent polarized monolayers was verified by measuring TER at different time intervals. TER (Ωcm2) = (Total resistance - Blank resistance) (Ω) ×Area (cm2). Because TER values often vary among individual NCM460 cultures, the electrical resistance value was recorded for each monolayer before and after the treatment, and the percentage in the decrease of TER from the baseline (%TER) was calculated.

3.4.2. Determination of dextran permeability in NCM460 monolayers
        To determine the dextran permeability, NCM460 cell monolayers were assayed by using a macromolecular conjugate probe, Alexa Fluor 647 dextran (10 kDa). Briefly, 0.2 ml DMEM containing conjugated dextran was added to the apical compartment of Transwells (Corning Costar Corp., MA, USA), and 0.4 ml of DMEM alone added to the basolateral compartment. After treatments as described above, samples (0.5 ml) collected from the basolateral compartment were placed into a 96-well plate (Corning Costar Corp.) and analyzed to determine their fluorescent intensity using the Odyssey infrared imaging system (LI-COR Biosciences, NE, USA) at a wavelength of 700 nm. Relative intensity (RI; the integrated intensities of treated samples relative to the integrated intensity of untreated samples) was calculated to indicate effect of the treatment.

3.4.3. Ussing chamber assay for determining the intestinal permeability measurement in isolated mouse colons
        IL-10^{-/-} and wild-type mice with or without treatment were sacrificed at 8 weeks after treatment as described above. Ussing chamber assay was performed as described elsewhere (49). Briefly, the segments of small intestine and colon were removed, and the mucosa was mounted in a Lucite chamber exposing the mucosal and serosal surfaces to 10 ml of oxygenated Krebs buffer (115 mM/L NaCl, 8 mM/L KCl, 1.25 mM/L $CaCl_2$, 1.2 mM/L $MgCl_2$, 2 mM/L KH_2PO_4, 225 mM/L $NaHCO_3$; pH 7.35). The buffer was maintained at 37°C by a heated water jacket and circulated with CO_2/O_2. Fructose (10 mM/L) was added to the serosal and mucosa sides. For measurement of the basal mannitol fluxes, 1 mM/L of mannitol with 370 KBO_r of ^3H was added to the mucosal side. The spontaneous transepithelial potential difference (PD) was determined, and the tissue was clamped at zero voltage by continuously introducing an appropriate short-circuit current with an automatic voltage clamp (DVC 1000 World Precision Instruments, FL, USA). Tissue ion resistance (1/G, where G is conductance) was calculated from the potential difference and short-circuit current according to Ohm's law.

3.4.4. Measurement of the intestinal permeability and colonic damage in mice

IL-10$^{-/-}$ and wild-type mice with or without treatment were sacrificed at 4-17 weeks after treatment as described above, and the intestinal paracellular permeability was determined as described (49). Briefly, once every week after the treatment, all mice were deprived of both food and water for 4 h, treated with an oral gavage of 0.2 ml sugar probe containing 12 mg of lactulose, 8 mg of mannitol and 6 mg of sucralose, and immediately housed in metabolic cages. After the collection of urine was complete, the animals were placed in their respective cages, and provided with food and water.

Urine sample was continuously collected from each animal for 22 h in a collection container and then treated with 100 µl of a 10% thymol solution (1.0 g/10 ml isopropanol) and paraffin oil (100 µl to prevent urine evaporation). Samples were frozen at -70°C until analysis. All sugars were quantified by ion exchange high-performance liquid chromatography (HPLC). Cellobiose was added as an internal standard, and the urine was filtered through a 0.4 µm filter and diluted as necessary. Samples were deionized and then injected onto a Dionex MA-1 ion exchange column (Dionex, CA, USA). Sugars were eluted with NaOH at a flow rate of 0.4 ml/min. Peaks were detected by HPLC with pulsed amperometric detection. Final data were reported as either the fractional excretion (for sucralose) to determine the colonic permeability or as a ratio of fractional excretion (for lactulose/mannitol) to determine the small intestinal permeability. Fractional excretion was defined as the fraction of the gavaged dose recovered in the urine sample, and the ratio of fractional excretion was defined as the ratio of the fraction of the gavaged dose of lactulose recovered in the urine sample over the fraction of the gavaged dose of mannitol recovered in the urine sample.

3.5. Determination of MIMP effects on TJ proteins and TJ ultrastructure *in vitro* and *in vivo*

3.5.1. Fluorescence staining and Western blotting for determining the distribution and expression of TJ proteins in NCM460 cell monolayers and mice

For fluorescence staining, NCM460 cells were cultured and the monolayers were treated as described above, and then the monolayers were fixed in acetone/methanol (1:1) at 0°C for 5 min. IL-10$^{-/-}$ and wild-type mice were fed and treated as described above; colonic tissue was fixed in 10% neutral-buffered formalin and embedded in paraffin and sectioned at 4 µm.

Fluorescence staining of TJ proteins was performed by using a method previously described (44). Briefly, samples prepared above were permeabilized in 0.2% Triton X-100, and incubated with a primary antibody and corresponding FITC conjugated specific secondary antibody in 3% nonfat milk. The fluorescence was visualized by confocal laser scanning microscopy (CLSM, Bio-Rad MRC 1024; Bio-Rad, CA, USA). Fluorescence at the intercellular junctions was quantitated by densitometry.

For Western blotting, NCM460 cells and mice were treated as described above. The protein samples from NCM460 cells and the colonic tissues of mice were prepared for sodium dodecyl sulfate polyacrylamide gel electrophoresis (SDS-PAGE) as described previously (44, 46). SDS-PAGE was performed according to standard laboratory techniques with a discontinuous gradient, 5% (w/v) stacking gel and a 10% (w/v) separating gel, in a Miniprotean II (Bio-Rad Laboratories, CA, USA). Briefly, samples were mixed with loading buffer containing SDS and mercaptoethanol, boiled for 3 min, centrifuged, and loaded onto the SDS-PAGE gel for separation. Molecular weights of samples were determined by comparing mobility with known marker proteins. One set of gels was stained with Coomassie brilliant blue R-250, and another set was transferred to PVDF membrane (Millipore, MA, USA) in a semidry electroblotter (Bio-Rad Laboratories) for 120 min at 100 V. The membrane was washed three times (20 min each) with PBS containing 0.1% Tween-20 (PBS-T buffer). After blocking overnight in Tris-buffered saline containing 0.05% Tween-20 (TBS-T) and 5% dry powdered milk, membranes were washed three times for 5 min each with TBS-T and incubated with corresponding primary antibodies for 2 h at room temperature. After three washes with TBS-T, the membranes were incubated for 1 h with corresponding HRP-conjugated secondary antibodies. The membrane was washed three times (60 min each) with PBS-T buffer. The TJ proteins were tested by using enhanced chemiluminescence (ECL kit; Pierce, IL, USA) according to the manufacturer's instructions.

3.5.2. Quantitative real time PCR for detecting the mRNA expression of TJ proteins in NCM460 cells and mice

mRNA expression of TJ proteins, including claudin-1, occludin, JAM-1, and ZO-1, was determined by quantitative real time PCR. After the treatment as described above, total RNA was isolated from NCM460 cells and colonic tissues of IL-10$^{-/-}$ and wild-type mice by using the Trizol reagent (Gibco Brl, USA) as previously described (50), followed by DNase I treatment. The quantity and quality of RNA was verified with the ratio of absorbance values at 260 and 280 nm, and by visualization of the bands on agarose gels. For each sample, 600 ng mRNA was used in reverse transcription reaction (iScript kit from BioRad Laboratories) according to the manufacturer's specifications. Further analysis of mRNA levels of each group was performed by real time PCR with a light-cycling system (LightCycler; Roche Diagnostics GmbH, Mannheim, Germany). Sequences of the primers used are compiled in Table 2. The level of mRNA expression was expressed as the ratio of the mean reading of the experimental group over that of the control group for NCM460 cells or wild-type group for mice.

3.5.3. Transmission electron microscopy for the observation of tight junctions in NCM460 cell monolayers and mice

NCM460 monolayers and the colonic tissues from the IL-10$^{-/-}$ and wild-type mice treated as described above were prepared for transmission electron microscopy (TEM). Briefly, live NCM460 cells (1×10^6 cfu) on the intact MillicellTM inserts or resected colonic tissues were rinsed with Dulbecco's PBS (D-PBS) and fixed with freshly

Functional characterization of MIMP

Table 2. Primers used for real time polymerase chain reaction amplification for genes encoding tight junction proteins in NCM460cells and mice

Gene	Forward primer (5'-3')	Reverse primer (5'-3')
NCM460 cell		
Occluding	GCAGCTACTGGACTCTACG	ATGGGACTGTCAACTCTTTC
Claudin-1	GTGCCTTGATGGTGGTTG	TGTTGGGTAAGAGGTTGT
JAM-1	GATGTGCCTGTGGTGCTG	GCTCTGCCTTGAGATAAGAA
ZO-1	AAGAGTGAACCACGAGAC	TCCGTGCTATACATTGAG
Mouse		
Occluding	AGTGCTGGTTCAGGAGTT	TGGAAAGGTCTAGTGGGT
Claudin-1	GATTTCCTCCCATCCAGC	ACCATGTTAGCCTGTGCC
JAM-1	AAAGACCGTGCTGAGATG	CTATGATGCCGCTTATGTT
ZO-1	TCCCTCCTCTGATACCTT	TGTCGTGCTCACTAAACTG

Table 3. Experimental grouping of dendritic cells

Group	Descriptions
Control	Cells with no treatments
L. plantarum	Cells treated with L. plantarum
MIMP	Cells treated with MIMP
L. plantarum +AZN-D1	Cells treated with L. plantarum and AZN-D1 simultaneously
L. plantarum +EDTA	Cells treated with L. plantarum and EDTA simultaneously
MIMP+AZN-D1	Cells treated with MIMP and AZN-D1 simultaneously
MIMP+ EDTA	Cells treated with MIMP and EDTA simultaneously

prepared 2.5% glutaraldehyde, 1.8% paraformaldehyde in cacodylate buffer (0.1 M, pH 7.4), post-fixed in 1% osmium tetroxide, dehydrated in a graded ethanol and propylene oxide series and embedded in Epon (Shell, Chemical Co., U.S.A.). Thin sections were obtained by an ultramicrotome (Reichert-Jung Ltd, Wetzlar, Germany) and stained with uranyl acetate and lead citrate, and then observed under a FEI TECNAI G2F20 electron microscope (FEI Ltd, OR, USA).

3.6. Determination of MIMP effects on DC-mediated immune responses
3.6.1. Flow cytometry for determining DC adhesion, maturation and Th1/Th2 differentiation
In the experiments, AZN-D1, a neutralizing antibody against DC-SIGN, Ca^{2+} chelator EDTA, and polyclonal antibodies against MIMP were used in different groups where appropriate (Table 3).

To determine the levels of adhesion of *L. plantarum* or MIMP to iDCs, *L. plantarum* and MIMP were labeled with FITC as described above, and incubated with iDCs at various ratios (from 10 to 1,000 cfu of *L. plantarum* per iDC or 0.01 μg/ml to 1 μg/ml of MIMP) in 1 mL medium containing approximately 5×10^4 iDCs, with or without AZN-D1 (20 μg/mL) or EDTA (10 mM). Then, DCs were analyzed by FACS flow cytometry.

To investigate the effect of MIMP on Th1/Th2 differentiation of iDCs, LPS (10 ng/mL, for non-uniform Th1/Th2 response) and PGE_2 (1 μg/mL, for Th2 response) were included as positive controls. Breifly, after treatment of iDCs (average of n = 5 donors) with *L. plantarum* (100 cfu of *L. plantarum* per iDC) or MIMP (0.1 μg/ml) at 37°C for 2 days, DCs were washed and incubated with prime T cells (utologous CD45RA+/CD4+ T cells) with a ratio of 1:4 (DCs:T cells) with or without AZN-D1 or EDTA. On day five, recombinant IL-2 (10 units/mL) was added, and the cells were cultured for the next 7-10 days. To determine cytokine production by T cells, quiescent T cells were re-

stimulated once daily for 6 h from day 12 to day 15 with 10 ng/mL phorbol 12-myristate 13-acetate and 1 μg/mL ionomycin. After 1 h, 1 μg/mL brefeldin A was added to the T cells. Cells were fixed in 2% paraformaldehyde, permeabilized with 0.5% saponin and stained with anti-human IFN-γ-FITC and anti-human IL-4-phycoerythrin. Single cell production of IL-4 and IFN-γ was determined by intracellular flow cytometric analysis (18).

3.6.2. Western blotting, fluorescence staining, and enzyme-linked immunosorbent assays (ELISA) for detecting MIMP binding to DC-SIGN of iDCs
For Western blotting, DC-SIGN-Fc was separated by SDS-PAGE; the transferred membrane was treated with 0.001 to 10 μg/ml MIMP and AZN-D1 or EDTA was added at the concentration of 0.1 μg. For the assay of DC, MIMP served as "primary antibody", while the HRP-labeled mucin was "secondary antibody".

For fluorescence staining, iDCs cells were incubated with *L. Plantarum* (100 cfu per iDC) or MIMP (0.1 μg/ml), which was labeled with the FITC according to the manufacturer's instructions (Pierce, IL, USA), with or without AZN-D1 (20 μg/mL) and EDTA (10 mM), at 37°C for 45 min, spotted onto poly(L)-lysine-coated glass slides, and stained by incubation with 4-Di-10-ASP.

For ELISA, goat anti-human antibodies (4 μg/ml) were used to coat plates for 1 h at 37°C. *L. plantarum*, MIMP and D-mannose were coated on designated NUNC maxisorb plates (Roskilde, Denmark) overnight at room temperature. Plates were blocked with 1% BSA, DC-SIGN-Fc (1 μg/mL) added, and then incubated at room temperature for 2 h in the presence or absence of AZN-D1 or EDTA. DC-SIGN-Fc adhesion was detected by using a secondary goat anti-human IgG antibodies conjugated with peroxidase.

3.6.3. ELISA for the determination of cytokine production by DCs

For cytokine measurements, iDCs were incubated with *L. plantarum* (10 to 1,000 cfu of *L. plantarum* per 1 iDC), MIMP (0.01 μg/ml), LPS (10 ng/mL), or no supplement for 2 days at 37°C. DC supernatants were harvested after the incubation, and human anti-inflammatory cytokines, IL-10, IL-6 and pro-inflammatory cytokine, IL-1β, were detected by ELISA with CytoSets ELISA kits (Biosource, Camarillo, CA, USA) according to the manufacturer's instructions; human pro-inflammatory cytokine, IL-12p70, was detected as described previously (51).

3.7. Determination of MIMP effects on colonic inflammation in IL-10$^{-/-}$ mice

3.7.1. Histological examination of colonic inflammation

Animals were treated as described above. Upon sacrifice, the whole colon was harvested from each and fixed in 10% phosphate-buffered formalin. These samples were embedded in paraffin *in toto*, sectioned at 4 μm, and stained with hematoxylin & eosin for light microscopy examination. The colons were histologically examined in a blind fashion by the same pathologists (J Huang and Shao-Hua Fei), simultaneously. Each segment of the colon (cecum, ascending, transverse, and descending colon) was assigned a histological score ranging from 0 to 4 based on the criteria adapted from (52). The sum of these scores provided a total colonic inflammatory score ranging from 0 (no change in any segment) to a maximum of 16 (grade 4 lesions in all four segments) per mouse.

3.7.2. Determination of mucosal cytokine and myeloperoxidase (MPO) concentrations

After treatment as described above, animals were sacrificed at age of 17 weeks. Colonic organ cultures were prepared from each group of IL-10$^{-/-}$ mice and wild-type mice. Because of the patchy nature of colitis in IL-10$^{-/-}$ mice, whole colons were removed, flushed with PBS, and a quarter of the tissue was cut longitudinally and resuspended in RPMI 1640 medium supplemented with 10% FBS, penicillin (100 U/mL), and streptomycin (100 μg/mL) in tissue culture plates (Falcon 3046; Becton Dickinson Labware, NJ, USA). After incubation at 37°C in 5% CO_2 for 24 h, the supernatants were harvested and stored at -70°C until analysis. Tumor necrosis factor-alpha (TNF-α), interferon-gamma (IFN-γ) and MPO levels in the cell supernatants were measured using ELISA kits (Cell Sciences).

3.8. Statistical analysis

The data were expressed as mean ± standard deviation (SD) when normally distributed, or median (range) when abnormally distributed. Statistical analyses were completed by using SPSS 10.0 system (SPSS Inc., IL, USA). SD between multiple groups was assumed to satisfy a normal distribution. Data were analyzed by one-way ANOVA on condition of homogeneity of variance. When the data did not satisfy the assumption of normal distribution, the ranks were transformed into the normal scores and the test statistics were calculated using analysis of one-way ANOVA. Dunnett-t test was used for multiple comparison of experimental and control groups. To examine differences between two experimental groups, the Student-Newman-Keuls (SNK) t test was employed for two sets of data or variables between two groups. A P value of < 0.05 was considered to be statistically significant.

4. RESULTS

4.1. MIMP effects on intestinal permeability *in vitro* and *in vivo*

4.1.1. MIMP prevents EIEC/EPEC-induced decrease of TER in NCM460 cells

Transepithelial electrical resistance (TER) in the NCM460 cell monolayers was found to be significantly decreased in response to infection with EIEC/EPEC, as compared with uninfected control cells (Figures 1A & 1B). However, the EIEC/EPEC-induced TER decrease was prevented by the simultaneous treatment of *L. plantarum* and MIMP. Treatment with anti-MIMP antibody inhibited the effect of MIMP on EIEC/EPEC-induced decrease in TER (Figures 1A & 1B).

4.1.2. MIMP inhibits increased macromolecular permeability of NCM460 cell monolayers in response to EIEC/EPEC

EIEC/EPEC exhibited a marked enhancing effect on permeability, as compared with the uninfected control cells. However, this effect was attenuated by the co-treatment of MIMP (Figures 1C & 1D). Again, anti-MIMP antibody increased the permeability, and blocked the inhibitory effect of MIMP on EIEC/EPEC-induced permeability (Figures 1C & 1D).

4.1.3. MIMP prevents the increase in intestinal permeability in IL-10$^{-/-}$ mice

By using the Ussing chamber assay, the *in vitro* effect of MIMP in reducing small intestinal permeability in 8-week old mouse tissues was evidenced. In *L. plantarum*, MIMP and AT-1001 groups, the small intestinal permeability to mannitol significantly decreased whereas TER significantly increased, as compared with the milk group of IL-10$^{-/-}$ mice (P<0.001; Figures 2A & 2B). Similar results were observed in colonic tissues. Colonic permeability to mannitol increased in the IL-10$^{-/-}$ mice with a corresponding decrease in TER, both of which were prevented by *L. plantarum*, MIMP and AT-1001 (P<0.001; Figures 2C & 2D).

An increased small intestinal permeability was indicated *in vivo* by the increased ratio of lactulose/mannitol observed in the IL-10$^{-/-}$ mice at age of 4 weeks and onwards, as compared with the wild-type mice (Figure 3A). Oral daily administration of pure milk containing *L. plantarum*, MIMP or AT-1001 for 4 weeks was effective in decreasing small intestinal permeability in IL-10$^{-/-}$ mice, and the effect was more evident at the age of 8 weeks when the small intestinal permeability returned to the normal level (Figure 3A).

In addition, sucralose excretion was measured weekly from 4 to 17 weeks to assess colonic permeability. IL-10$^{-/-}$ mice had a significantly increased intestinal
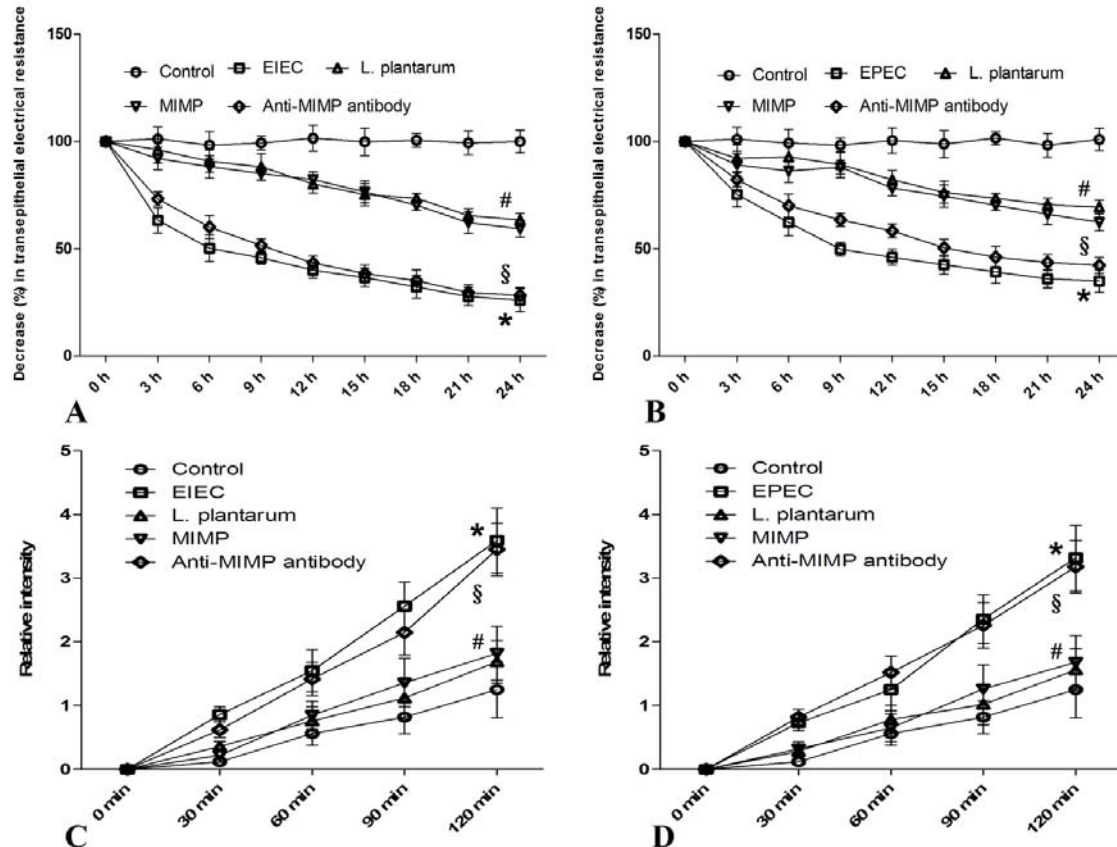
Figure 1. L. plantarum and MIMP inhibit the increased permeability and macromolecular permeability through NCM460 cells induced by enteroinvasive E. coli (EIEC, A) or enteropathogenic E. coli (EPEC, B). (A), After infection with EIEC for 24 h, the transepithelial electrical resistance (TER) of NCM460 monolayers was decreased by approximately 73.96%, compared with the value in the control group (480 $\Omega\cdot cm^2$ vs. 125 $\Omega\cdot cm^2$). However, TER of EIEC-infected NCM460 monolayers, when simultaneously co-incubated with L. plantarum or MIMP was decreased by only 36.46% (to 305 $\Omega\cdot cm2$) or 40.63% (to 285 $\Omega\cdot cm2$), but the values were significantly greater than those in EIEC-infected NCM460 monolayers. When NCM460 monolayers were pre-treated with anti-MIMP antibodies for 2 h before EIEC infection and co-cultured with MIMP, TER was decreased by 71.67% (to 136$\Omega\cdot cm2$). (B), Similar results were obtained in the experiments with EPEC. (C), After infection with EIEC for 120 min, the relative intensity (RI) was significantly increased in the EIEC group, compared with the control group (3.59 ± 0.51 vs. 1.25 ± 0.44). However, the RI was only 1.69 ± 0.39 and 1.82 ± 0.42, respectively, in L. plantarum and MIMP groups. In the group pre-treated with anti-MIMP antibodies, RI was 3.45 ± 0.41. (D), Similar results were obtained in the experiments with EPEC. The data at each time point represent the mean value ± standard deviation (SD) obtained from four individual NCM460 monolayers. *, P<0.001, compared with control group; #, P<0.001, compared with corresponding EIEC or EPEC group; §, P<0.001, compared with MIMP group.

permeability, as compared to the wild-type animals. Treatment of *L. plantarum*, MIMP or AT-1001 had no significant effects on the intestinal permeability until week 10. After week 10, oral administration of pure milk containing *L. plantarum*, MIMP or AT-1001 daily for 4 weeks was effective in decreasing colonic permeability in IL-10^{-/-} mice (Figure 3B).

**4.2. MIMP effects on TJ proteins and TJ ultrastructure**
in vitro
4.2.1. MIMP prevents decrease in the expression and rearrangement of TJ proteins and F-actin as detected by fluorescence staining

The intensity of fluorescence of TJ proteins and cytoskeletal F-actin were relatively low, and the

fluorescence was distributed throughout the NCM460 cell monolayers infected with EIEC (Figure 4A) or with EPEC (Figure 4B). However, in NCM460 cell monolayers treated with *L. plantarum* or MIMP, the intensity and the distribution of fluorescence appeared similar to that in the control cells. Anti-MIMP antibody inhibited the ability of *L. plantarum* and MIMP to maintain the intensity and the distribution of fluorescence to the normal level (Figure 4).

Fluorescence staining of colon revealed the effect of MIMP on the TJ and F-actin. In the tissue of wild-type mice, TJ proteins, including claudin-1, occludin, JAM-1 and ZO-1, were continuously distributed with particularly bright spots along the membrane of the cells (Figure 5). In IL-10^{-/-} mice fed with milk, the fluorescence of undermined
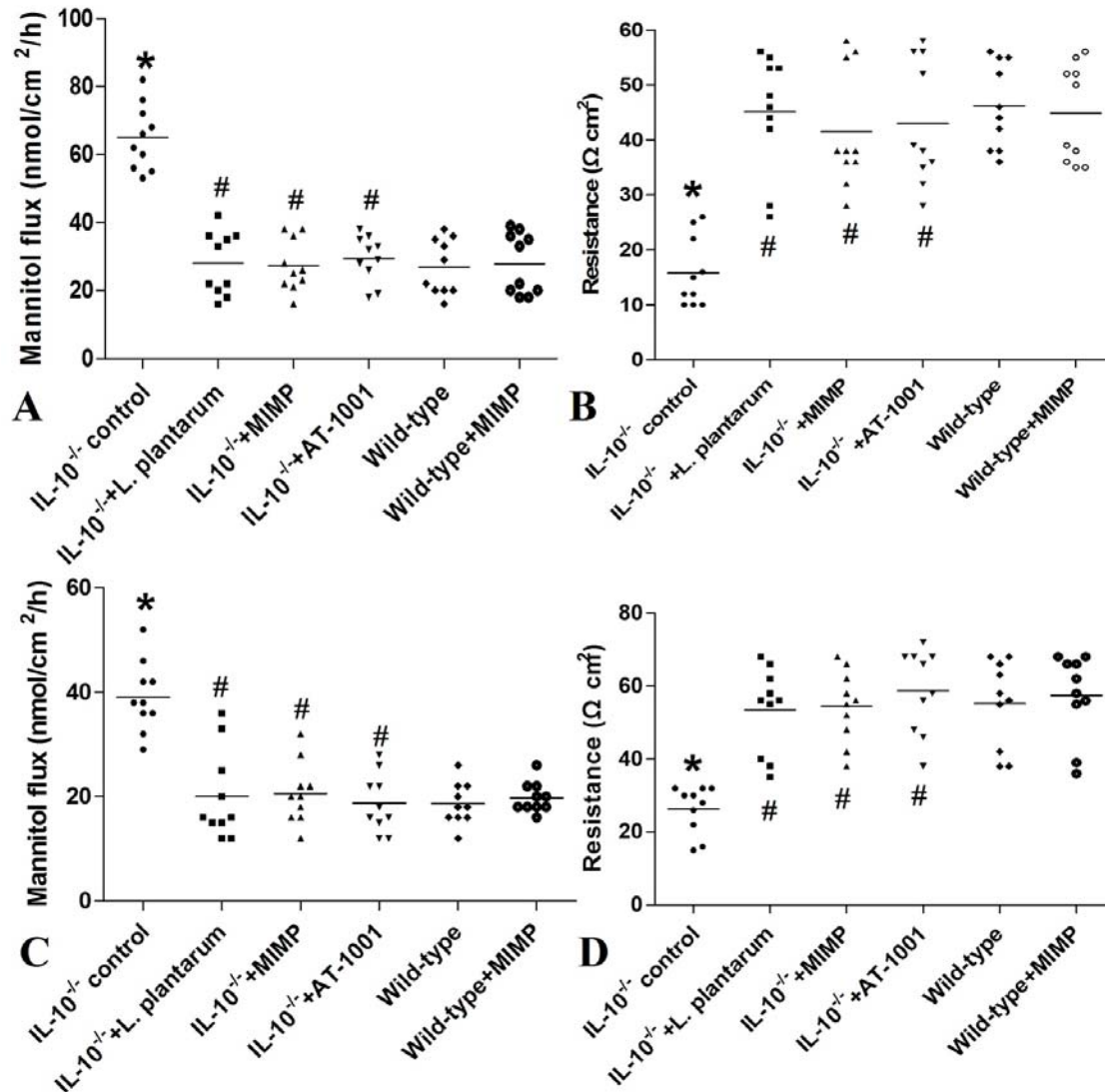
Figure 2. L. plantarum and MIMP reduce small intestinal and colonic permeability in IL-10$^{-/-}$ mice at 8 weeks of age. (A), Mannitol flux of small intestine measured in the Ussing chamber is increased in the IL-10$^{-/-}$ mice, compared with wild-type mice (P<0.05). This increase is not observed in L. plantarum, MIMP and AT-1001 groups. (B), The transepithelial electrical resistance (TER) of small intestine is reduced in the IL-10$^{-/-}$ mice, compared with TER in wild type mice (P<0.05), which is not observed in L. plantarum, MIMP and AT-1001 groups. (C), Colonic mannitol flux is significantly increased in the IL-10$^{-/-}$ mice, compared with that in wild-type mice. This increase is not observed in L. plantarum, MIMP and AT-1001 groups (all, P<0.05). (D), TER of the colon is decreased in IL-10$^{-/-}$ mice, compared with the wild-type group. However, this increase is not observed in the L. plantarum, MIMP and AT-1001 groups. The data represent the mean value ± standard deviation (SD) obtained from 10 mice *, P<0.001, compared with wild-type mice; #, P<0.001, compared with IL-10$^{-/-}$ mice fed with pure milk.

TJ proteins was faint and distributed throughout (Figure 5); by contrast, in *L. plantarum*-, MIMP- or AT-1001-treated mice, the intensity of fluorescence and distribution was similar to that observed in the wild-type mice (Figure 5).

4.2.2. MIMP prevents the decrease in the expression of TJ proteins as detected by Western blotting

Western blotting of epithelial whole-cell protein extracts showed that the expression of TJ proteins, including claudin-1, occludin, JAM-1 and ZO-1, were decreased in NCM460 cells infected with EIEC (Figures

6A1 & 6A2) or EPEC (Figures 6B1 & 6B2), compared with the control cells (both, *P* < 0.001). However, in NCM460 cells treated with *L. plantarum* and MIMP, the expression of TJ proteins remained at levels similar to the control cells. Again, anti-MIMP antibody abolished the enhancing effect of both *L. plantarum* and MIMP on the expression of TJ proteins (Figures 6A1-6B2).

The expression of TJ proteins, claudin-1, occludin, JAM-1 and ZO-1, in colonic tissues was significantly reduced in IL-10$^{-/-}$ mice fed with milk, when compared with the wild-
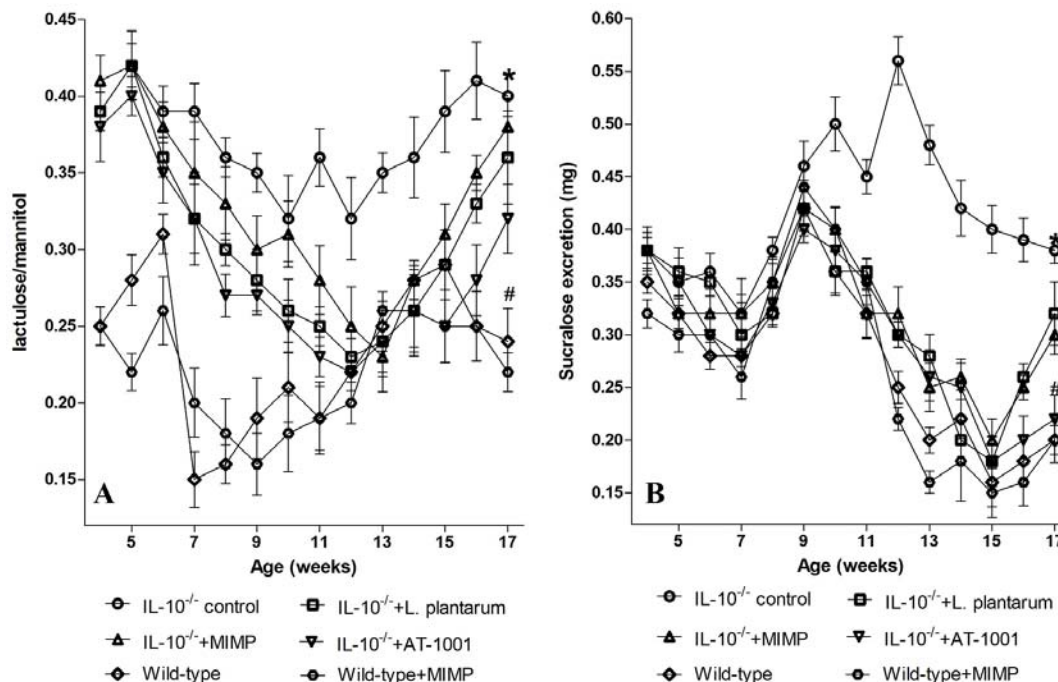
Figure 3. L. plantarum and MIMP reduce *in vivo* small intestinal and colonic permeability in IL-10$^{-/-}$ mice at different time points as detected by intestinal permeability. The ratio of lactulose/mannitol excretion is significantly greater in all IL-10$^{-/-}$ mice, compared with that in wild-type mice at baseline (i.e. aged 3.5 weeks) (A). Sucralose excretion in IL-10$^{-/-}$ mice is increased at baseline, compared with that in wild-type mice. Following the course, IL-10$^{-/-}$ mice fed with pure milk exhibit continuous and even higher sucralose excretion, compared with IL-10$^{-/-}$ mice treated with L. plantarum, MIMP and AT-1001 (B). The data represent the mean value ± standard deviation (SD) obtained from 10 mice in each group. *, $P<0.001$, compared with the negative control; #, $P<0.001$, compared with IL-10$^{-/-}$ mice fed with pure milk.

type mice ($P<0.001$) (Figures 6C1 & 6C2). However, after treatment with *L. plantarum*, MIMP or AT-1001, the expression of these proteins was significantly increased (Figures 6C1 & 6C2), when compared with IL-10$^{-/-}$ mice fed with milk ($P<0.001$).

4.2.3. MIMP prevents the decrease in the expression of TJ proteins as detected by quantitative RT-PCR

There was a significant decrease in the mRNA expression of TJ proteins, including claudin-1, occludin, JAM-1 and ZO-1, in NCM460 cells infected with EIEC or EPEC, as compared with the uninfected control cells (Figures 7A & 7B). Treatment with *L. plantarum* and MIMP resulted in mRNA expression increased to levels similar to those in the uninfected control cells (Figures 7A & 7B).

Quantitative RT-PCR using the colonic tissues of IL-10$^{-/-}$ and wild-type mice revealed a significant increase in mRNA expression of TJ proteins in IL-10$^{-/-}$ mice treated with *L. plantarum*, MIMP or AT-1001, compared with IL-10$^{-/-}$ mice fed with milk (all, $P<0.001$; Figure 7C).

4.2.4. MIMP prevents the destruction of the TJ structure as detected by TEM

In the control cells, the diameter of TJ structure was measured as 25-38 nm and concentrated at the top of the membrane between the adjacent NCM460 cells (Figure

8A). The TJ structure appeared irregular, and disrupted TJs and microvilli, a marked increase in the intercellular gap, vacuolization, chromatin condensation, and even epithelial apoptosis were observed in cells infected with EIEC/EPEC, as compared with the uninfected control cells (Figure 8A). However, treatment with *L. plantarum* and MIMP prevented the destructive effect of EIEC/EPEC on the TJ structure. Anti-MIMP antibodies abolished the effect of both *L. plantarum* and MIMP on the TJ structure (Figure 8A).

TEM examination demonstrated that in the colonic tissues of wild-type mice, TJ structure concentrated at the top of the membrane. In IL-10$^{-/-}$ mice fed with milk, similar structural and functional deficits as in the EIEC/EPEC infected NCM460 cells were observed. In IL-10$^{-/-}$ mice treated with *L. plantarum*, MIMP or AT-1001, the TJ structure was similar to that in the wild-type mice (Figure 8B).

**4.3. MIMP effects on DC-mediated immune responses**
4.3.1. MIMP adheres to iDCs as detected by flow cytometry

After the interaction with FITC-labeled *L. plantarum* or MIMP, fluorescence was increased in a concentration-dependent manner. Fluorescence was detected when the ratio was more than 10 cfu of *L. plantarum* per iDC and strengthened following the increase

Functional characterization of MIMP
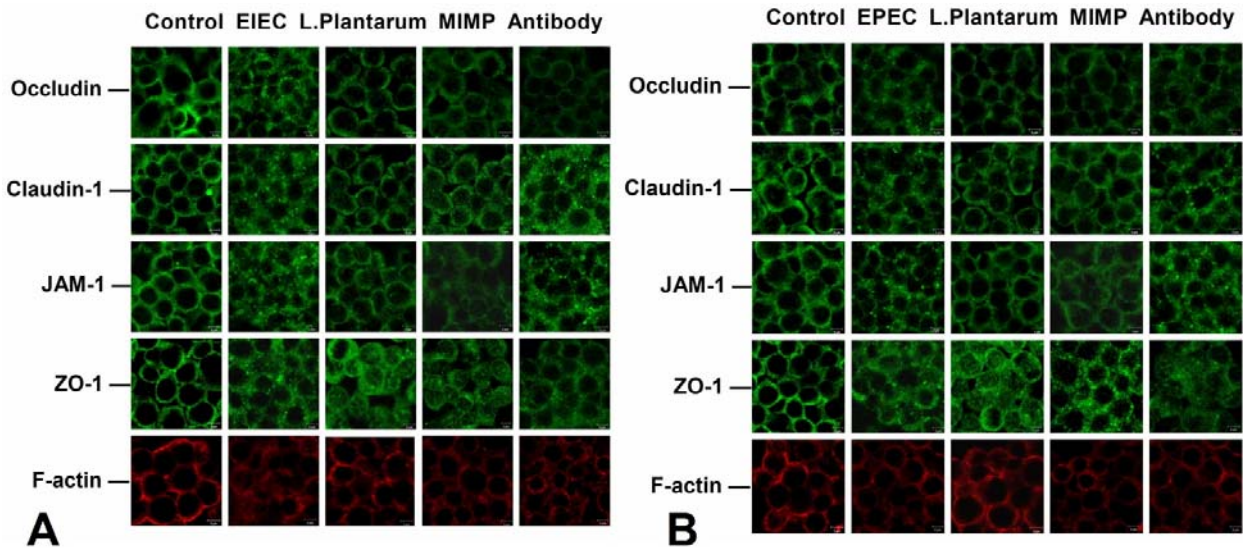
Figure 4. Protective effect of L. plantarum and MIMP on the rearrangement of TJ proteins and F-actin in NCM460 cells as detected by fluorescence staining. (A) EIEC induces injury of TJ and F-actin, which is prevented by MIMP. In the control cells, TJ-associated proteins, including claudin-1, occludin, JAM-1 and ZO-1, and F-actin were distributed throughout as evidenced by bright green spots along the membrane of the cells (lane 1). In the EIEC and anti-MIMP antibody groups, the intensity of the stain was reduced and distribution was disordered (lanes 2 and 5). However, in the L. plantarum and MIMP groups, the intensity and distribution of the proteins were similar to those in the control group (Lanes 2 and 3). (B) Similar results were found in EPEC groups. Images were collected in 1 μm increments beginning at the apical aspect of the monolayers and optically sectioning to the basolateral membrane. Original magnification ×630.
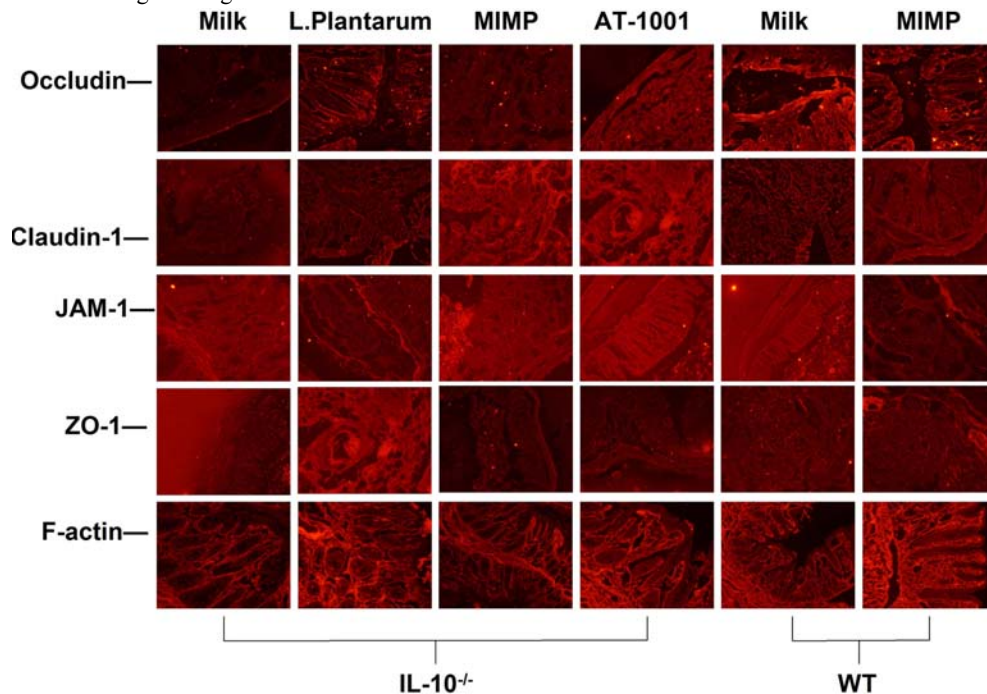
Figure 5. Protective effect of L. plantarum and MIMP on the rearrangement of TJ proteins and F-actin in IL-10$^{-/-}$ mice as detected by fluorescence staining. In IL-10$^{-/-}$ mice fed with pure milk, the fluorescence of TJ proteins, including claudin-1, occludin, JAM-1 and ZO-1, and F-actin is faint, and the distribution of the fluorescence is dispersed (Line 1). In wild-type mice and wild-type mice treated with oral gavage of MIMP, TJ proteins and F-actin are distributed throughout, as evidenced by bright green spots along the membrane of the cells in the tissue (Lines 5 and 6). In the L. plantarum, MIMP and AT-1001 groups, the intensity of TJ proteins and F-actin is enhanced and the distribution of fluorescence becomes regular, similar to the wild-type mice (Lanes 2-4). Original magnification ×2400.
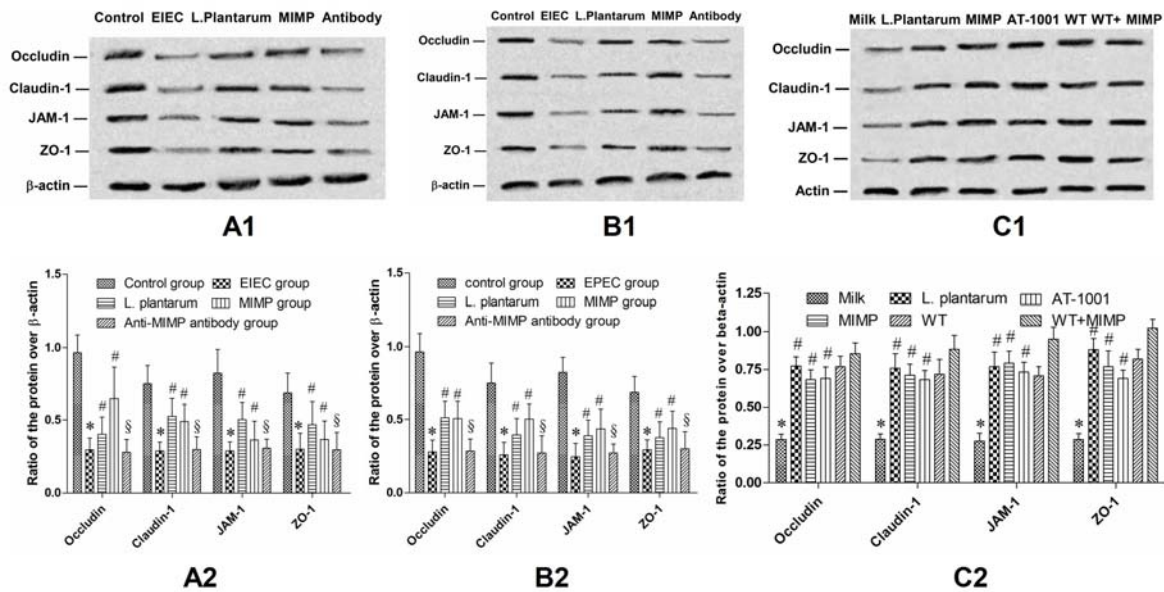
Figure 6. L. plantarum and MIMP prevent the decrease in the expression of tigh junction (TJ) proteins in NCM460 cells and IL-10^{-/-} mice as detected by Western blotting. The expression of TJ proteins, including claudin-1, occludin, JAM-1 and ZO-1, in the control group had a high expression. However, in the EIEC group, TJ proteins were significantly decreased in EIEC and antibody groups, compared with the control group, but not observed in the MIMP group (A1, B1). Similar results were obtained with EPEC (A2, B2). The data at each time point represent the mean value ± standard deviation (SD) obtained from four individual NCM460 monolayers. *, P<0.001, compared with control group; #, P<0.001, compared with corresponding EIEC or EPEC group; §, P<0.001, compared with MIMP group. (C) L. plantarum and MIMP enhance the expression of tight junction (TJ) proteins in IL-10^{-/-} mice as detected by Western blotting. In IL-10^{-/-} mice fed with pure milk, the expression of TJ proteins are reduced, compared with wild-type mice. However, the expression of TJ proteins in L. plantarum, MIMP and AT-1001 groups is similar to that in the wild-type mice (C1). Quantitative analysis of the expression of TJ proteins in different groups (C2). The data represent the mean value ± standard deviation (SD) obtained from 10 mice. *, P<0.001, compared with wild-type mice; #, P<0.001, compared with IL-10^{-/-} mice fed with pure milk.

in the ratio of *L. plantarum* to iDCs. Moreover, fluorescence was detected even at the smallest ratio for MIMP (i.e. 0.01 μg/ml). These findings indicate the ability of *L. plantarum* and MIMP to adhere to iDCs. However, EDTA and polyclonal anti-MIMP antibodies inhibited the adhesion ability for both *L. plantarum* and MIMP (Figure 9).

4.3.2. MIMP adheres to iDCs by binding to DC-SIGN as detected by Western blotting, fluorescence staining, and ELISA

The role of a C-type lectin receptor (CLR), DC-SIGN, in the interactions between L. plantarum or MIMP and iDCs was next evaluated. The DC-SIGN-Fc interaction with MIMP was assessed by Western blotting, and strong adhesion was detected at concentrations ranging from 0.01 to 10 μg/ml of MIMP. AZN-D1 or the Ca2+ chelator EDTA inhibited this adhesion at the concentration of 0.1 μg/ml (Figure 10A). Interaction of MIMP and DC-SIGN was also supported by visual fluorescence staining (Figure 10B), which was quenched by the treatment of AZN-D1and EDTA.

In addition, ELISA indicated strong binding of *L. plantarum* and MIMP to the DC-SIGN-Fc. Addition of

AZN-D1 blocked the binding completely. Binding of *L. plantarum* and MIMP to DC-SIGN-Fc was also significantly reduced by the presence of EDTA (Figure 10C).

4.3.3. MIMP promotes the production of anti-inflammatory cytokines in DCs as detected by ELISA

The expression of anti-inflammatory (IL-10 and IL-6) and pro-inflammatory (IL-12p70 and IL-1β) cytokines during the maturation of iDCs was significantly influenced by the concentrations of *L. plantarum* or MIMP. The levels of IL-10 and IL-6, as well as IL-1β, were increased in DCs incubated with *L. plantarum* or MIMP, with the highest ratios (i.e. 100:1 for *L. plantarum* and 0.1 μg/ml for MIMP) producing the highest levels of IL-10 and IL-6 (*P*<0.001; Figures 11A, 11B & 11D). IL-12p70 expression was up-regulated after incubation with *L. plantarum* or MIMP, but the effect was not concentration-dependent for either *L. plantarum* or MIMP, with the lowest ratios (10:1 for *L. plantarum* and 0.01 μg/ml for MIMP) producing the highest levels (Figure 11C). The effects of *L. plantarum* and MIMP on cytokine production were inhibited by treatment with AZN-D1 or EDTA (Figure 11).
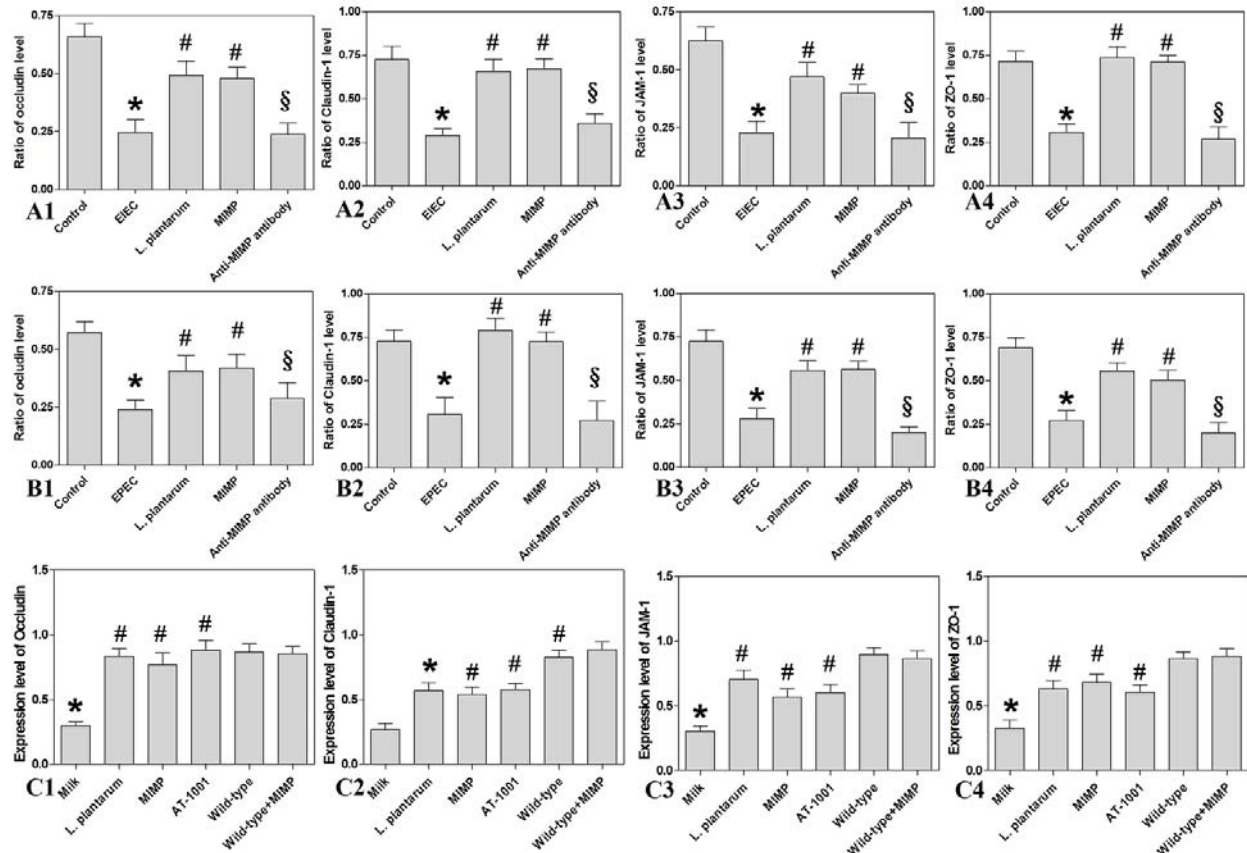
Figure 7. Protective effect of L. plantarum and MIMP on mRNA expression of tight junction (TJ) proteins in NCM460 cells and IL-10^{-/-} mice as detected by real-time PCR. The mRNA expression of TJ proteins, including occluding (A1), claudin-1 (A2), JAM-1 (A3) and ZO-1 (A4), is decreased in EIEC and antibody groups, compared to the control group. However, in L. plantarum and MIMP groups, the mRNA expression of the proteins is similar to those in the control group (A). Similar results were obtained with EPEC (B). The data at each time point represent the mean value ± standard deviation (SD) obtained from individual NCM460 monolayers. *, P<0.001, compared with control group; #, P<0.001, compared with corresponding EIEC or EPEC group; §, P<0.001, compared with MIMP group. (C) Protective effect of L. plantarum and MIMP on mRNA expression of tight junction (TJ) proteins in IL-10^{-/-} mice as detected by real time PCR. mRNA expression of TJ proteins is decreased in the IL-10^{-/-} group fed with pure milk, compared with the wild-type group. However, mRNA expression of the proteins in L. plantarum, MIMP and AT-1001 groups is similar to that in the wild-type group. The data represent the mean value ± standard deviation (SD obtained from 10 mice. *, P<0.001, compared with wild-type mice; #, P<0.001, compared with IL-10^{-/-} mice fed with pure milk.

4.3.4. MIMP induces DCs to mediate Th2 predominant differentiation as detected by flow cytometry

MIMP was found to induce more IL-4-producing T cells than interferon-gamma (IFN-γ)-producing T cells (18% IL-4-producing T cells *vs.* 9% IFN-γ-producing T cells; *P*<0.001). Treatment with AZN-D1 resulted in a non-uniform response in T cell differentiation (8% IFN-γ-producing T cells and 10% IL-4-producing T cells). Also, treatment with EDTA showed similar results (18% IFN-γ and 19% IL-4 *vs.* 9% IFN-γ and 9% IL-4) (Figure 12).

4.4. MIMP effects on colonic inflammation in IL-10^{-/-} mice
4.4.1. MIMP affects the expression of cytokines and myeloperoxidase (MPO) and ameliorates colonic inflammation

At 17 weeks of age, IFN-γ and tumor necrosis factor-alpha (TNF-α) secretion in the colon of IL-10^{-/-} mice was found to be increased. However, the levels were significantly reduced in response to treatment with *L. plantarum*, MIMP or AT-1001, compared with the IL-10^{-/-} mice fed with milk (all, *P*<0.001; Figures 13A1 & 13A2). Neutrophil infiltration in the colon, as measured by tissue MPO, showed similar profiles (Figure 13A3).

A similar attenuation effect was observed histologically. Marked inflammation was observed in the IL-10^{-/-} mice fed with pure milk. However, treatment with *L. plantarum*, MIMP or AT-1001 showed a significant reduction in the severity of the inflammation (Figure 13B). Similarly, the histological scores in IL-10^{-/-} mice treated with *L. plantarum*, MIMP and AT-1001 were significantly lower than in IL-10^{-/-} mice fed with milk (all, *P*<0.001; Figure 13C).
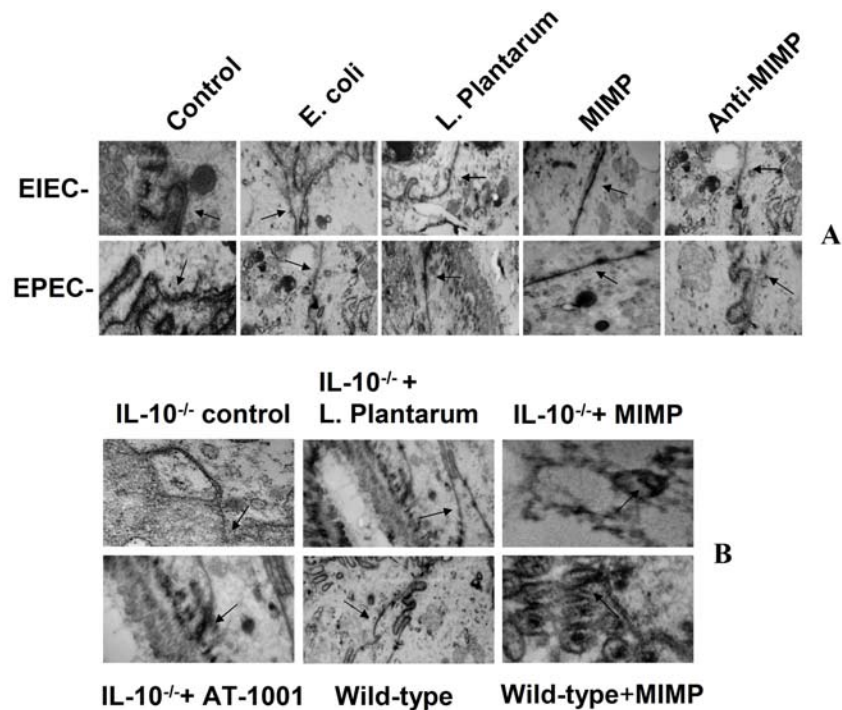
Figure 8. L. plantarum and MIMP prevent tight junction (TJ) structure from destruction in NCM460 cells and IL-10$^{-/-}$ mice as detected by transmission electronic microscopy. (A), In the control NCM460 cells, the TJ structures are located at the top of the membrane between two adjacent cells (arrows). The TJ structures appear to be perturbed (arrows) in EIEC/EPEC and antibody groups. However, the destruction is not observed in L. plantarum group and MIMP groups and the TJ structure was located at the top of the membrane between two adjacent cells (arrows) as it was in the control group. (B), In wild-type mice with or without MIMP treatment (arrows), the TJ structures are located at the top of the membrane between the adjacent NCM460 cells, with the diameter of TJ structure being measured as 25-38 nm. In IL-10$^{-/-}$ mice fed with pure milk (arrows), the TJ structures appear to be irregular. However, in the L. plantarum, MIMP and AT-1001 groups (arrows), the TJ structures appear similar to those in the wild-type group.
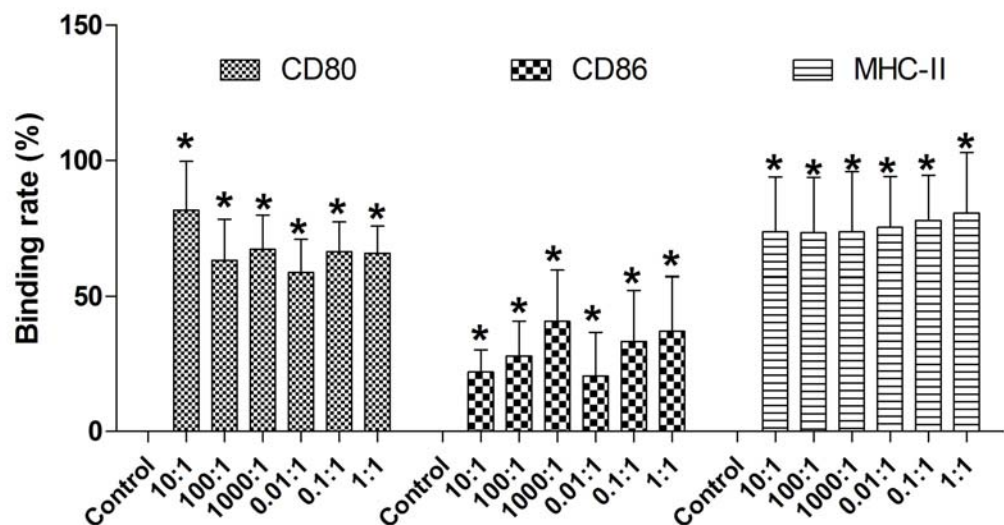
Figure 9. L. plantarum and MIMP adheres to immature dendritic cells (iDCs) as analyzed by FACScan. Adherence occurs in a concentration-dependent manner. However, after addition of EDTA and AZN-D1, the adhesion rates decrease significantly. Low concentration (L), medium concentration (M), and high concentration (H) means 10, 100, 1,000 cfu of *L. plantarum* or 0.01, 0.1, 1 μg/ml of MIMP per iDC. The data represent the mean value ± standard deviation *, P<0.001, compared with the control group; #, P<0.001, compared with * group.
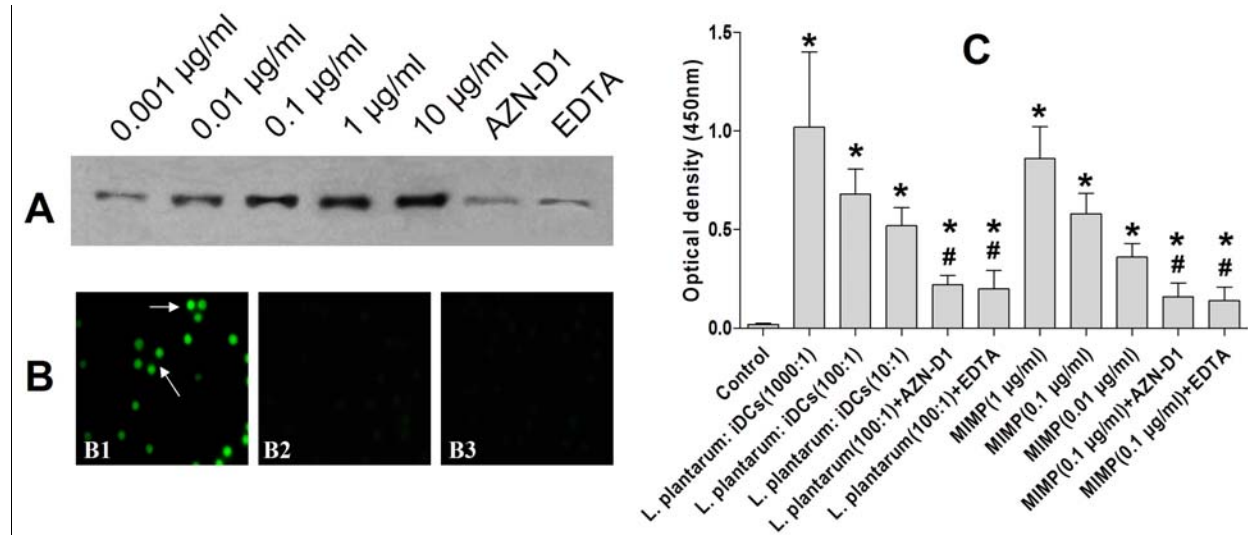
Figure 10. L. plantarum and MIMP bind to DC-SIGN of immature dendritic cells (iDCs) as detected by Western blotting, visual fluorescence staining, and enzyme-linked immunosorbent assay (ELISA). MIMP starts to bind to DC-SIGN of iDCs at the concentration of 0.001 µg/ml and the strength is concentration-dependent as detected by Western blotting; AZN-D1 and EDTA inhibit the binding at the concentration of 0. 1 µg/ml (A). Microscope analysis of visual fluorescence staining shows binding of MIMP to DCs (arrows, B1). However, the bindings were blocked by addition of AZN-D1 (B2), or EDTA (B3). In addition, the biding rates were also evaluated by ELIAS. L. plantarum and MIMP bind strongly to the DC-SIGN-Fc as indicated by the optical density (OD) at 450 nm, which is concentration-dependent; however, the addition of AZN-D1 or EDTA blocks the binding (C). The data represents the mean value ± standard deviation (SD) obtained from duplicate measurements of three independent experiments. *, P<0.001, compared with the control group; #, P<0.001, compared with corresponding L. plantarum and MIMP groups.

5. DISCUSSION

It has been reported that probiotics, such as *L. plantarum*, have beneficial effects in patients with intestinal diseases such IBD (53); however, the mechanisms by which *L. plantarum* exerts these effects have not been fully elucidated (54). In our previous study (our simultaneously submitted manuscript), we identified MIMP as the smallest actively functional domain responsible for the adhesion property of *L. plantarum* to gastric mucin and NCM460 cells. In the present study, we further characterized the functions of MIMP in NCM460 cells, DCs and IL-10$^{-/-}$ mice. We found that MIMP, as well as *L. plantarum,* decreased intestinal permeability by increasing the expression and TJ proteins and restoring TJ protein distribution and the TJ ultrastructure. We also observed that MIMP and *L. plantarum* interacted with DCs by binding DC-SIGN, and induced DCs to mediate a Th2 immune response. Moreover, MIMP and *L. plantarum* attenuated colonic inflammation.

Based on these findings and those obtained from our previous studies (44, 46-47), we propose that *L. plantarum* exerts its therapeutic effects in patients with IBD mainly through MIMP in at least three aspects. NCM460, iDCs and the mice used in different experiments for the characterization of MIMP functions are outlined in Figure 14.

First, MIMP plays an important role in protection of intestinal barrier function, including intestinal permeability and TJ proteins and ultrastructure. EIEC and EPEC have the ability to disrupt the epithelial TJ structure, including distribution of claudin-1, occludin, JAM-1, and ZO-1, resulting in decreased TER and increased permeability to macromolecules, while *L. plantarum* might prevent and ameliorate the pathogen-induced redistribution of TJ proteins (44, 46). In the present study, we further observed that MIMP exerted a similar effect to that of *L. plantarum* in protecting the epithelial barrier (i.e. NCM460 monolayers) against the disruption caused by EIEC or EPEC. MIMP was able to attenuate the pathogen-induced decrease in TER, and inhibited the increase in the macromolecular permeability. Previous studies have demonstrated that IL-10$^{-/-}$ mice do not suffer from colitis in the absence of intestinal bacterial flora, and one or more components of bacteria in the enormously complex flora may have the ability to trigger the development of inflammation in the susceptible mucosal immune system (49, 55). Increased intestinal permeability has been considered as the critical sign of perturbation in intestinal barrier function, which contributes to the development of colitis, while reducing permeability can attenuate the barrier defect and prevent colitis (56-57). In the present study, MIMP prevented the increase in either small intestinal or colonic

Functional characterization of MIMP
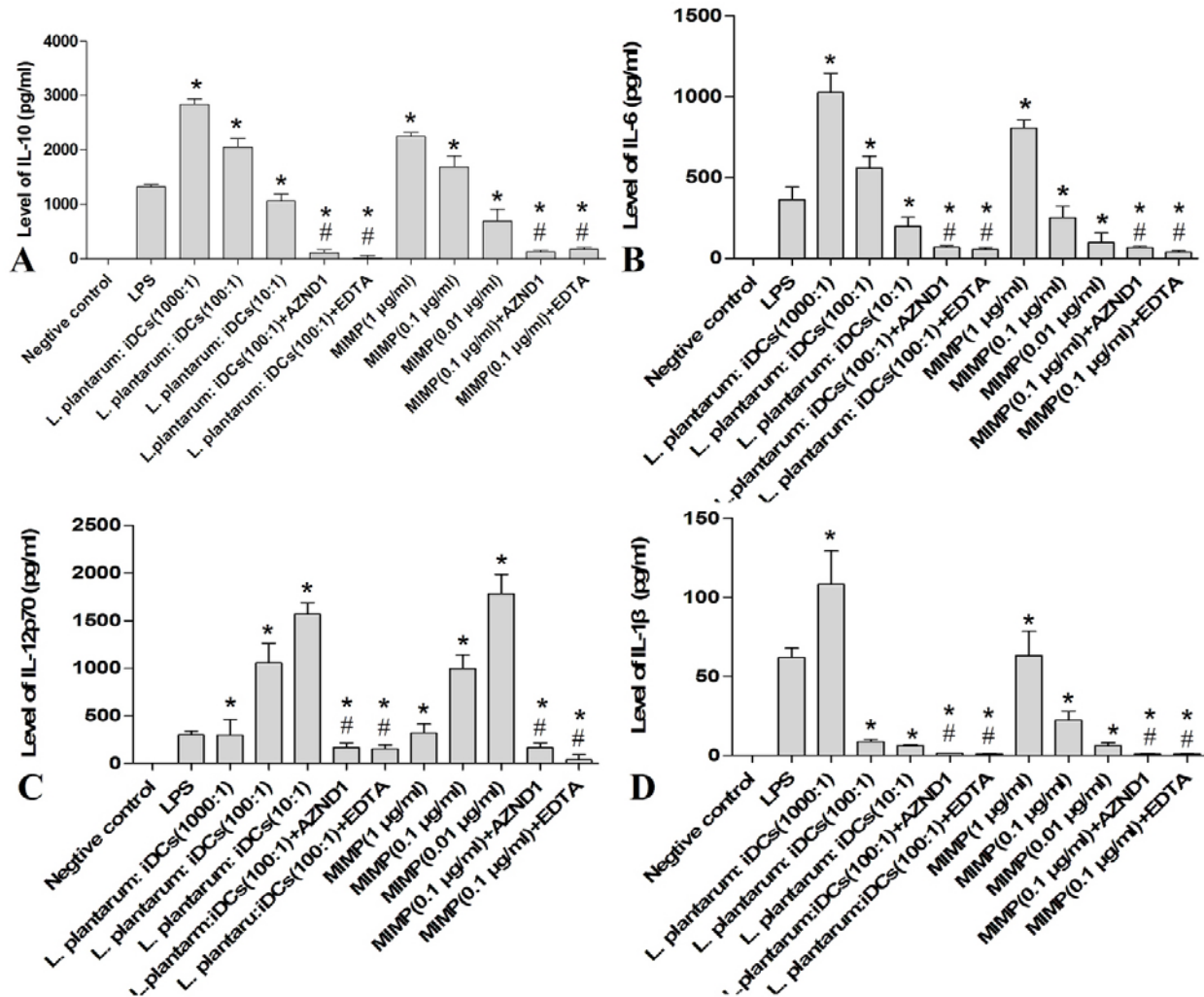
Figure 11. L. plantarum and MIMP induce cytokine production of immature dentritic cells (iDCs). L. plantarum and MIMP induce iDCs to produce increased levels of IL-6, IL-10 and IL-1β, in a concentration-dependent manner (A, B, D). L. plantarum and MIMP also up-regulate the expression of IL-12p70, but with the lowest concentration exhibiting the strongest effect (C). However, all effects on the cytokine production are inhibited by the addition of AZN-D1 or EDTA. The data represent the mean value ± standard deviation (SD) obtained from duplicate measurements of three independent experiments. *, P<0.001, compared with the negative control; #, P<0.001, compared with corresponding L. plantarum and MIMP groups.

permeability in IL-10$^{-/-}$ mice. Furthermore, we found that MIMP also prevented the decrease in the expression and rearrangement of TJ proteins and F-actin, as well as the destruction of the TJ structure, in both NCM460 cells and IL-10$^{-/-}$ mice. Therefore, *L. plantarum* may exert its protective effect through its active functional component, MIMP. Indeed, similar protective effects have also been reported for some functional components of Lactobacilli (14, 16, 58).

Second, MIMP plays an important role in DC-mediated immune responses by inducing the maturation and production of anti-inflammatory cytokines of DCs, and guiding DC-mediated Th1/Th2 differentiation. In the present study, we first observed that MIMP as well as *L.*

plantarum adhered to iDCs and stimulated maturation of iDCs by up-regulating MHC-II and activating the expression of the co-stimulatory molecules CD80 and CD86. However, Ca^{2+} chelator EDTA and polyclonal anti-MIMP antibodies inhibited the adhesion ability for both *L. plantarum* and MIMP. We further detected that MIMP adhered to iDC by binding to a CLR, DC-SIGN, and the binding was inhibited by Ca^{2+} chelator EDTA. It has been shown that, CLRs, mainly expressed on DCs, recognize mannose- and fucose-containing glycans that are present on endogenous membranes and surfaces of bacteria or viruses, and thus contribute to immune responses (18, 59). Interestingly, the results of the present study indicate that CLRs also interacted with SLPs (e.g. MIMP) directly, which may play an important role in the
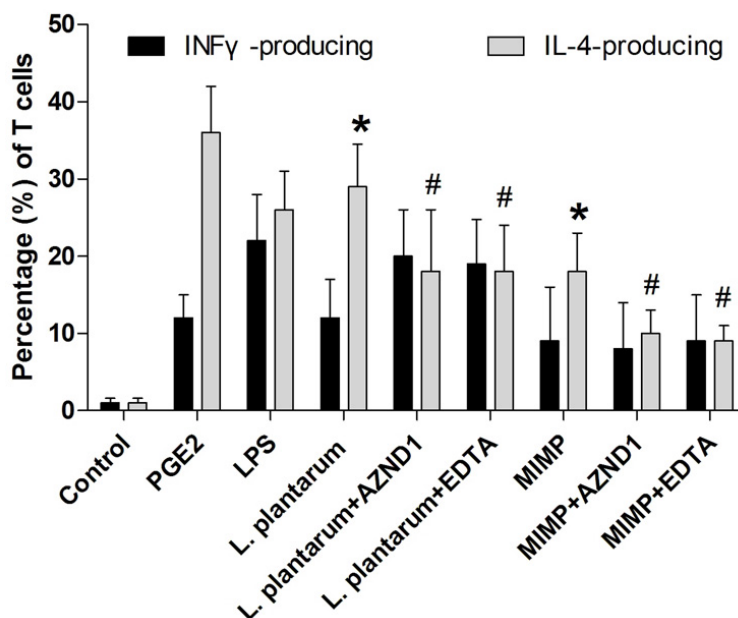
Figure 12. L. plantarum and MIMP induce DC-mediated Th2 polarization as detected by flow cytometry. L. plantarum and MIMP induce more IL-4 (Th2) compared with IFN-γ-producing T cells (Th1). However, the pre-treatment with AZN-D1 and EDTA results in a non-uniform T cell differentiation. The data represent the mean value ± standard deviation (SD) obtained from duplicate measurements of three independent experiments. *, $P<0.001$, compared with the IFN-γ-producing T cells; #, $P>0.001$, compared with IFN-γ-producing T cells. Functional characterization of MIMP, the domain within the integral membrane protein of Lactobacillus plantarum responsible for its adhesion to the intestinal epithelium

subsequent immune responses; however, in order to detail these mechanisms further investigation is required.

Furthermore, the findings from the present study suggest that MIMP promotes DCs to produce IL-10 and IL-6, key anti-inflammatory cytokines that maintain homeostasis of the gut flora and are responsible for the anti-inflammatory effects of probiotic cultures (30, 60) and inhibits the expression of the pro-inflammatory cytokine IL-12p70. Other probiotics such as *L. acidophilus*, *L. gasseri*, *L. johnsonii* and and *L. reuteri* can also bind to DC-SIGN and induce the production of anti-inflammatory cytokines (18, 30, 61). Moreover, the present study showed that MIMP induced DCs to mediate Th2 predominant differentiation. Therefore, MIMP is able to interact with and stimulate the function of DCs, and then regulate DC-mediated immune functions by interfering with pathogen-induced effects on the host immune system, thereby increasing immune response triggered by DC. It should be emphasized that the adhesion potency of DCs for *L. plantarum* was strengthened following the increase in the ratio of *L. plantarum* to iDCs, with the minimal ratio of 100 cfu of *L. plantarum* per 1 iDC. However, MIMP adhered to iDC even at the lowest concentration (i.e. 0.01 μg/ml) used in the experiment, suggesting MIMP possesses a very high potency in interacting with DCs.

Third, MIMP may directly exert anti-inflammatory effects in colonic mucosa by modulating local expression of cytokines and MPO, and reducing histological inflammatory severity. It has been reported that

colonic inflammation may not occur in IL-10$^{-/-}$ mice lacking intestinal bacterial flora and any component of the bacterial flora may trigger the development of inflammation in the colon (49, 55). Zonulin (ZO-1) is a protein in tight junctions between epithelial cells of the digestive tract, and plays an important role in maintaining the TJ structure. When the expression of zonulin is up-regulated, tight junctions would be opened, and the colonic permeability would be increased, leading to possible intestinal injury. AT-1001, a zonulin receptor antagonist, competitively inhibits the apical zonulin receptor, and thus has the ability to reduce the colonic permeability and protect the intestine from injury (49). However, no studies have been reported that investigate the role of a functional component of Lactobacillus towards the protection of colonic inflammation. Our present *in vivo* study demonstrated that, like AT-1001, MIMP affected cytokine and MPO expression and ameliorated colonic inflammation.

Intestinal barrier dysfunction occurs in patients with intestinal diseases such as intestinal infection and IBD. Currently, there is no effective treatment for IBD and the treatment for chronic intestinal infection is usually limited to supportive treatment, as use of antibiotics is associated with an increased risk of developing systemic complications (14, 62-63). It has been reported that probiotics are effective in prevention and treatment of intestinal barrier dysfunction (6-8); however, their clinical safety remains to be established (64). A few studies have indicated that some SLPs of Lactobacilli may protect

Functional characterization of MIMP
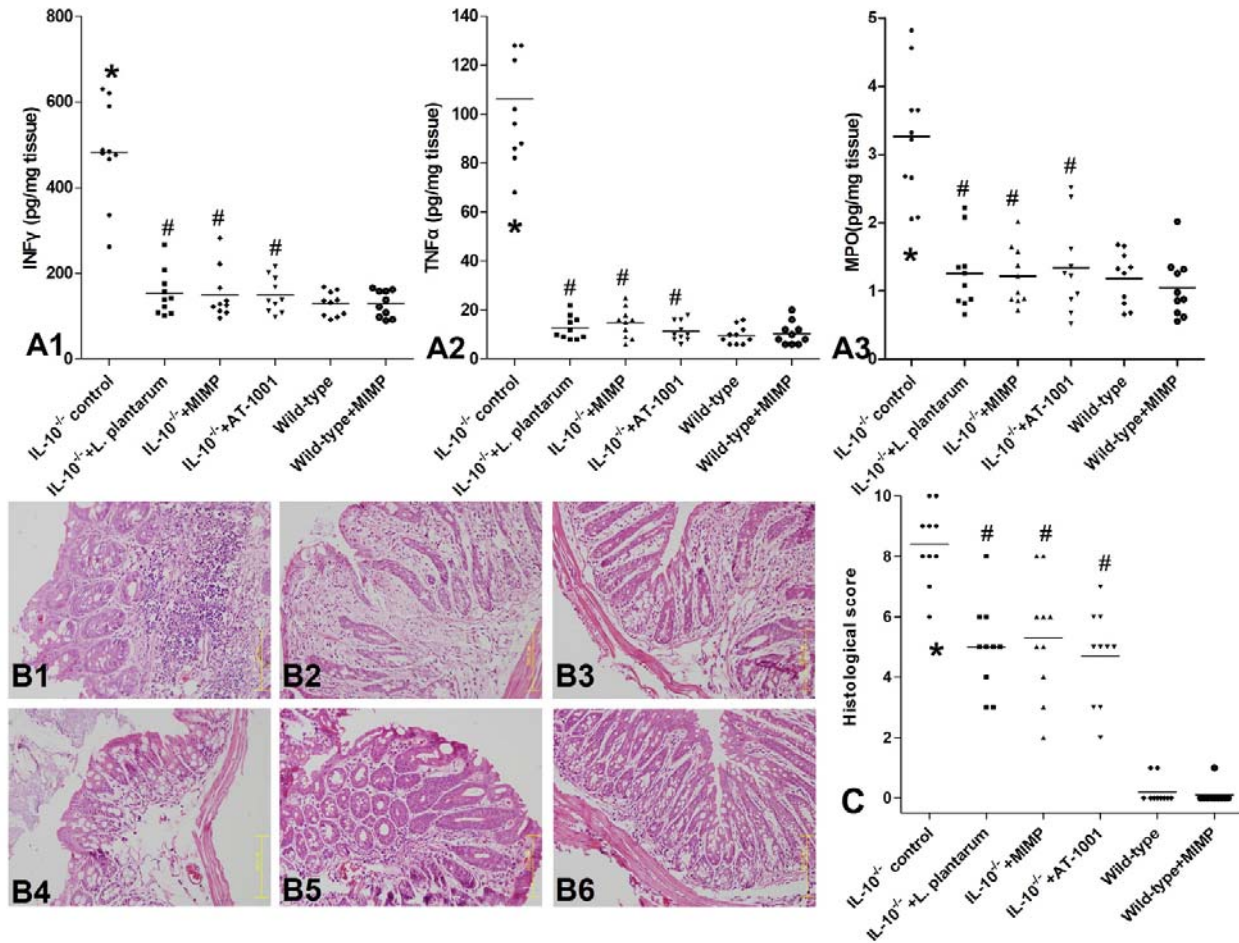
Figure 13. L. plantarum and MIMP down-regulate the expression of IFN-γ, TNFα and MPO in the colon, and attenuate colonic inflammation in IL-10$^{-/-}$ mice. The expression levels of IFN-γ, TNFα and MPO in the colon are significantly increased in IL-10$^{-/-}$ mice fed with pure milk, compared with wild-type mice. However, treatment with L. plantarum, MIMP and AT-1001 decrease the expression of IFN-γ, TNFα and MPO to the levels seen in wild-type (A1-A3). In addition, colonic inflammation is present in IL-10$^{-/-}$ mice (B1). The treatment with L. plantarum, MIMP and AT-1001 attenuates, but do not completely resolve the inflammation (B2-B4). L. plantarum, MIMP and AT-1001 groups had significantly decreased histological scores as compared to the pure milk group, however the scores were still higher than the wild-type group (C). The bars represent the mean value obtained from 10 mice in each group. *, $P<0.001$, compared with wild-type mice; #, $P<0.001$, compared with the IL-10$^{-/-}$ control group.

colonic epithelial cells from injury by pathogens (14, 58); however, the functional components of the SLPs and their effects have not been explored. Our present study broadens our current understanding of the domain in the SLP (i.e. IMP) of *L. plantarum* and its functional characteristics both *in vitro* and *in vivo*; although, studies with MIMP knockout *L. plantarum* are needed to further confirm our findings. Further investigation of the underlying molecular and cellular mechanisms such as cell signal transduction pathways is warranted, and is now in progress.
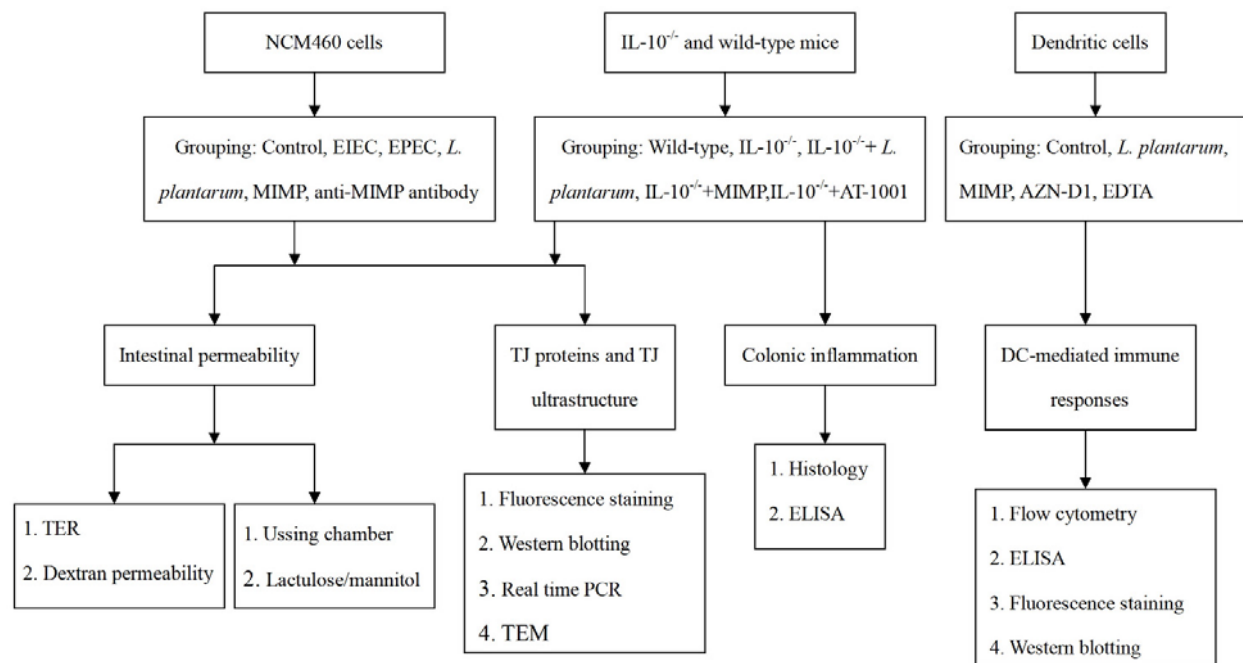
In conclusion, MIMP, as the adhesive domain of SLP on *L. plantarum*, reduces intestinal permeability. MIMP adheres to iDCs by binding to DC-SIGN, stimulates maturation of iDCs, and induces DCs to produce anti-inflammatory cytokines and to mediate Th2 differentiation. Moreover, MIMP stimulates the expression of anti-

inflammatory cytokines in colonic mucosa and attenuates colitis in IL-10$^{-/-}$ mice. These data indicate that MIMP is the main functional component of *L. plantarum* that contributes to its effects, and thus may be a potential therapeutic agent for intestinal diseases, such as inflammatory bowel disease.

6. ACKNOWLEDGMENT

Figure 14. Experimental flow chart.

7. REFERENCES

1. T. Matsuzaki, A. Takagi, H. Ikemura, T. Matsuguchi and T. Yokokura: Intestinal microflora: probiotics and autoimmunity. *J Nutr*, 137(3 Suppl 2), 798S-802S (2007)

2. K. Madsen, A. Cornish, P. Soper, C. McKaigney, H. Jijon, C. Yachimec, J. Doyle, L. Jewell and C. De Simone: Probiotic bacteria enhance murine and human intestinal epithelial barrier function. *Gastroenterology*, 121(3), 580-91 (2001)

3. A. Swidsinski, A. Ladhoff, A. Pernthaler, S. Swidsinski, V. Loening-Baucke, M. Ortner, J. Weber, U. Hoffmann, S. Schreiber, M. Dietel and H. Lochs: Mucosal flora in inflammatory bowel disease. *Gastroenterology*, 122(1), 44-54 (2002)

4. P. Lepage, J. Colombet, P. Marteau, T. Sime-Ngando, J. Dore and M. Leclerc: Dysbiosis in inflammatory bowel disease: a role for bacteriophages? *Gut*, 57(3), 424-5 (2008)

5. J. B. Kaper, J. P. Nataro and H. L. Mobley: Pathogenic Escherichia coli. *Nat Rev Microbiol*, 2(2), 123-40 (2004)

6. G. K. Makharia, A. Sood, V. Midha, V. Ahuja, D. K.

Singal, R. Arora, S. Seed, P. Goswami, C. De Simone, A. R. Saha and R. K. Tandon: A randomized, double-blind, placebo-controlled trial of a probiotic preparation, Vsl#3, for the treatment of mild to moderate active ulcerative colitis. *Gastroenterology*, 134(4), A99-A99 (2008)

7. E. Miele, F. Pascarella, E. Giannetti, L. Quaglietta, R. N. Baldassano and A. Staiano: Effect of a Probiotic Preparation (VSL# 3) on Induction and Maintenance of Remission in Children With Ulcerative Colitis. *American Journal of Gastroenterology*, 104(2), 437-443 (2009)

8. B. J. Rembacken, A. M. Snelling, P. M. Hawkey, D. M. Chalmers and A. T. R. Axon: Non-pathogenic Escherichia coli versus mesalazine for the treatment of ulcerative colitis: a randomised trial. *Lancet*, 354(9179), 635-639 (1999)

9. S. C. Ng, A. L. Hart, M. A. Kamm, A. J. Stagg and S. C. Knight: Mechanisms of Action of Probiotics: Recent Advances. *Inflammatory Bowel Diseases*, 15(2), 300-310 (2009)

10. A. Garcia-Lafuente, M. Antolin, F. Guarner, E. Crespo and J. R. Malagelada: Modulation of colonic barrier function by the composition of the commensal flora in the rat. *Gut*, 48(4), 503-7 (2001)

11. M. G. Gareau, J. Jury, G. MacQueen, P. M. Sherman and M. H. Perdue: Probiotic treatment of rat pups normalises corticosterone release and ameliorates colonic dysfunction induced by maternal separation. *Gut*, 56(11), 1522-8 (2007)

12. M. Rinkinen, E. Westermarck, S. Salminen and A. C.

Ouwehand: Absence of host specificity for *in vitro* adhesion of probiotic lactic acid bacteria to intestinal mucus. *Veterinary Microbiology*, 97(1-2), 55-61 (2003)

13. M. Horie, A. Ishiyama, Y. Fujihira-Ueki, J. Sillanpaa, T. K. Korhonen and T. Toba: Inhibition of the adherence of Escherichia coli strains to basement membrane by Lactobacillus crispatus expressing an S-layer. J Appl Microbiol, 92(3), 396-403 (2002)

14. K. C. Johnson-Henry, K. E. Hagen, M. Gordonpour, T. A. Tompkins and P. M. Sherman: Surface-layer protein extracts from Lactobacillus helveticus inhibit enterohaemorrhagic Escherichia coli O157:H7 adhesion to epithelial cells. *Cell Microbiol*, 9(2), 356-67 (2007)

15. S. Avall-Jaaskelainen, U. Hynonen, N. Ilk, D. Pum, U. B. Sleytr and A. Palva: Identification and characterization of domains responsible for self-assembly and cell wall binding of the surface layer protein of Lactobacillus brevis ATCC 8287. *BMC Microbiol*, 8, 165 (2008)

16. S. A. van Hijum, S. Kralj, L. K. Ozimek, L. Dijkhuizen and I. G. van Geel-Schutten: Structure-function relationships of glucansucrase and fructansucrase enzymes from lactic acid bacteria. *Microbiol Mol Biol Rev*, 70(1), 157-76 (2006)

17. J. M. Wells and A. Mercenier: Mucosal delivery of therapeutic and prophylactic molecules using lactic acid bacteria. *Nat Rev Microbiol*, 6(5), 349-62 (2008)

18. S. R. Konstantinov, H. Smidt, W. M. de Vos, S. C. Bruijns, S. K. Singh, F. Valence, D. Molle, S. Lortal, E. Altermann, T. R. Klaenhammer and Y. van Kooyk: S layer protein A of Lactobacillus acidophilus NCFM regulates immature dendritic cell and T cell functions. *Proc Natl Acad Sci U S A*, 105(49), 19474-9 (2008)

19. S. K. Mazmanian, C. H. Liu, A. O. Tzianabos and D. L. Kasper: An immunomodulatory molecule of symbiotic bacteria directs maturation of the host immune system. *Cell*, 122(1), 107-18 (2005)

20. Z. H. Liu, Y. L. Ma, T. Y. Shen, H. Q. Chen, Y. K. Zhou, P. Zhang, M. Zhang, Z. X. Chu and H. L. Qin: Identification of DC-SIGN as the receptor during the interaction of lactobacillus plantarum CGMCC 1258 and dendritic cells. *World J Microbiol Biotechnol*. (2010)

21. M. Mohamadzadeh, T. Duong, S. J. Sandwick, T. Hoover and T. R. Klaenhammer: Dendritic cell targeting of Bacillus anthracis protective antigen expressed by Lactobacillus acidophilus protects mice from lethal challenge. *Proc Natl Acad Sci U S A*, 106(11), 4331-6 (2009)

22. E. G. Pamer: Immune responses to commensal and environmental microbes. *Nat Immunol*, 8(11), 1173-8 (2007)

23. M. Rescigno, M. Urbano, B. Valzasina, M. Francolini, G. Rotta, R. Bonasio, F. Granucci, J. P. Kraehenbuhl and P. Ricciardi-Castagnoli: Dendritic cells express tight junction proteins and penetrate gut epithelial monolayers to sample bacteria. *Nat Immunol*, 2(4), 361-7 (2001)

24. J. P. Kraehenbuhl and M. Corbett: Immunology. Keeping the gut microflora at bay. *Science*, 303(5664), 1624-5 (2004) 303/5664/1624 [pii]

25. A. J. Macpherson and T. Uhr: Induction of protective IgA by intestinal dendritic cells carrying commensal bacteria. *Science*, 303(5664), 1662-5 (2004)

26. B. L. Kelsall and W. Strober: Distinct populations of dendritic cells are present in the subepithelial dome and T cell regions of the murine Peyer's patch. *J Exp Med*, 183(1), 237-47 (1996)

27. J. H. Niess, S. Brand, X. Gu, L. Landsman, S. Jung, B. A. McCormick, J. M. Vyas, M. Boes, H. L. Ploegh, J. G. Fox, D. R. Littman and H. C. Reinecker: CX3CR1-mediated dendritic cell access to the intestinal lumen and bacterial clearance. *Science*, 307(5707), 254-8 (2005)

28. S. J. van Vliet, J. den Dunnen, S. I. Gringhuis, T. B. Geijtenbeek and Y. van Kooyk: Innate signaling and regulation of Dendritic cell immunity. *Curr Opin Immunol*, 19(4), 435-40 (2007)

29. H. H. Smits, A. Engering, D. van der Kleij, E. C. de Jong, K. Schipper, T. M. van Capel, B. A. Zaat, M. Yazdanbakhsh, E. A. Wierenga, Y. van Kooyk and M. L. Kapsenberg: Selective probiotic bacteria induce IL-10-producing regulatory T cells *in vitro* by modulating dendritic cell function through dendritic cell-specific intercellular adhesion molecule 3-grabbing nonintegrin. *J Allergy Clin Immunol*, 115(6), 1260-7 (2005)

30. M. Mohamadzadeh, S. Olson, W. V. Kalina, G. Ruthel, G. L. Demmin, K. L. Warfield, S. Bavari and T. R. Klaenhammer: Lactobacilli activate human dendritic cells that skew T cells toward T helper 1 polarization. *Proc Natl Acad Sci U S A*, 102(8), 2880-5 (2005)

31. K. Robinson, L. M. Chamberlain, M. C. Lopez, C. M. Rush, H. Marcotte, R. W. Le Page and J. M. Wells: Mucosal and cellular immune responses elicited by recombinant Lactococcus lactis strains expressing tetanus toxin fragment C. *Infect Immun*, 72(5), 2753-61 (2004)

32. A. C. Moss, P. Anton, T. Savidge, P. Newman, A. S. Cheifetz, J. Gay, S. Paraschos, M. W. Winter, M. P. Moyer, K. Karalis, E. Kokkotou and C. Pothoulakis: Urocortin II mediates pro-inflammatory effects in human colonocytes via corticotropin-releasing hormone receptor 2alpha. *Gut*, 56(9), 1210-7 (2007)

33. H. Kim, E. Kokkotou, X. Na, S. H. Rhee, M. P. Moyer, C. Pothoulakis and J. T. Lamont: Clostridium difficile toxin A-induced colonocyte apoptosis involves p53-dependent p21(WAF1/CIP1) induction via p38 mitogen-activated protein kinase. *Gastroenterology*, 129(6), 1875-88 (2005)

34. H. W. Koon, D. Zhao, Y. Zhan, M. P. Moyer and C. Pothoulakis: Substance P mediates antiapoptotic responses in human colonocytes by Akt activation. *Proc Natl Acad Sci U S A*, 104(6), 2013-8 (2007)

35. Z. Liu, P. Zhang, Y. Ma, H. Chen, Y. Zhou, M. Zhang, Z. Chu and H. Qin: Lactobacillus plantarum prevents the development of colitis in IL-10-deficient mouse by reducing the intestinal permeability. *Mol Biol Rep*. (2010)

36. S. C. Kim, S. L. Tonkonogy, C. A. Albright, J. Tsang, E. J. Balish, J. Braun, M. M. Huycke and R. B. Sartor: Variable phenotypes of enterocolitis in interleukin 10-deficient mice monoassociated with two different commensal bacteria. *Gastroenterology*, 128(4), 891-906 (2005)

37. B. C. Sydora, S. M. Macfarlane, J. W. Walker, A. L. Dmytrash, T. A. Churchill, J. Doyle and R. N. Fedorak: Epithelial barrier disruption allows nondisease-causing bacteria to initiate and sustain IBD in the IL-10 gene-deficient mouse. *Inflamm Bowel Dis*, 13(8), 947-54 (2007)

38. R. Kuhn, J. Lohler, D. Rennick, K. Rajewsky and W. Muller: Interleukin-10-deficient mice develop chronic enterocolitis. *Cell*, 75(2), 263-74 (1993)

39. C. Nicaise, D. Prozzi, E. Viaene, C. Moreno, T. Gustot, E. Quertinmont, P. Demetter, V. Suain, P. Goffin, J. Deviere and P. Hols: Control of acute, chronic, and constitutive hyperammonemia by wild-type and genetically engineered Lactobacillus plantarum in rodents. *Hepatology*, 48(4), 1184-1192 (2008)

40. J. Ewaschuk, R. Endersby, D. Thiel, H. Diaz, J. Backer, M. Ma, T. Churchill and K. Madsen: Probiotic bacteria prevent hepatic damage and maintain colonic barrier function in a mouse model of sepsis. *Hepatology*, 46(3), 841-50 (2007)

41. M. Roselli, A. Finamore, S. Nuccitelli, P. Carnevali, P. Brigidi, B. Vitali, F. Nobili, R. Rami, I. Garaguso and E. Mengheri: Prevention of TNBS-Induced Colitis by Different Lactobacillus and Bifidobacterium Strains Is Associated with an Expansion of gamma delta T and Regulatory T Cells of Intestinal Intraepithelial Lymphocytes. *Inflammatory Bowel Diseases*, 15(10), 1526-1536 (2009)

42. H. S. Lee, S. Y. Han, E. A. Bae, C. S. Huh, Y. T. Ahn, J. H. Lee and D. H. Kim: Lactic acid bacteria inhibit proinflammatory cytokine expression and bacterial glycosaminoglycan degradation activity in dextran sulfate sodium-induced colitic mice. *International Immunopharmacology*, 8(4), 574-580 (2008)

43. M. Schultz, C. Veltkamp, L. A. Dieleman, W. B. Grenther, P. B. Wyrick, S. L. Tonkonogy and R. B. Sartor: Lactobacillus plantarum 299V in the treatment and prevention of spontaneous colitis in interleukin-10-deficient mice. *Inflammatory Bowel Diseases*, 8(2), 71-80 (2002)

44. H. Qin, Z. Zhang, X. Hang and Y. Jiang: L. plantarum prevents enteroinvasive Escherichia coli-induced tight junction proteins changes in intestinal epithelial cells. *BMC Microbiol*, 9, 63 (2009)

45. H. L. Qin, J. J. Zheng, D. N. Tong, W. X. Chen, X. B. Fan, X. M. Hang and Y. Q. Jiang: Effect of Lactobacillus plantarum enteral feeding on the gut permeability and septic complications in the patients with acute pancreatitis. *Eur J Clin Nutr*, 62(7), 923-30 (2008)

46. M. Zhang, X. Q. Wang, Y. K. Zhou, Y. L. Ma, T. Y. Shen, H. Q. Chen, Z. X. Chu and H. L. Qin: Effects of oral Lactobacillus plantarum on hepatocyte tight junction structure and function in rats with obstructive jaundice. *Mol Biol Rep* (2009)

47. Z. X. Chu, H. Q. Chen, Y. L. Ma, Y. K. Zhou, M. Zhang, P. Zhang and H. L. Qin: Lactobacillus plantarum Prevents the Upregulation of Adhesion Molecule Expression in an Experimental Colitis Model. *Dig Dis Sci* (2009)

48. F. Sallusto and A. Lanzavecchia: Efficient presentation of soluble antigen by cultured human dendritic cells is maintained by granulocyte/macrophage colony-stimulating factor plus interleukin 4 and downregulated by tumor necrosis factor alpha. *J Exp Med*, 179(4), 1109-18 (1994)

49. M. C. Arrieta, K. Madsen, J. Doyle and J. Meddings: Reducing small intestinal permeability attenuates colitis in the IL10 gene-deficient mouse. *Gut*, 58(1), 41-8 (2009)

50. V. Lelievre, Z. Hu, J. Y. Byun, Y. Ioffe and J. A. Waschek: Fibroblast growth factor-2 converts PACAP growth action on embryonic hindbrain precursors from stimulation to inhibition. *J Neurosci Res*, 67(5), 566-73 (2002)

51. K. P. van Gisbergen, M. Sanchez-Hernandez, T. B. Geijtenbeek and Y. van Kooyk: Neutrophils mediate immune modulation of dendritic cells through glycosylation-dependent interactions between Mac-1 and DC-SIGN. *J Exp Med*, 201(8), 1281-92 (2005)

52. D. J. Berg, N. Davidson, R. Kuhn, W. Muller, S. Menon, G. Holland, L. Thompson-Snipes, M. W. Leach and D. Rennick: Enterocolitis and colon cancer in interleukin-10-deficient mice are associated with aberrant cytokine production and CD4(+) TH1-like responses. *Journal of Clinical Investigation*, 98(4), 1010-20 (1996)

53. G. Reid, J. Jass, M. T. Sebulsky and J. K. McCormick: Potential uses of probiotics in clinical practice. *Clin Microbiol Rev*, 16(4), 658-72 (2003)

54. S. Santosa, E. Farnworth and P. J. Jones: Probiotics and their potential health claims. *Nutr Rev*, 64(6), 265-74 (2006)

55. M. C. Arrieta, L. Bistritz and J. B. Meddings: Alterations in intestinal permeability. *Gut*, 55(10), 1512-20 (2006)

56. P. Mannon: Gut permeability and colitis. *Gastroenterology*, 137(2), 732-4 (2009)

57. T. S. Olson, B. K. Reuter, K. G. Scott, M. A. Morris, X. M. Wang, L. N. Hancock, T. L. Burcin, S. M. Cohn, P. B. Ernst, F. Cominelli, J. B. Meddings, K. Ley and T. T. Pizarro: The primary defect in experimental ileitis originates from a nonhematopoietic source. *J Exp Med*, 203(3), 541-52 (2006)

58. X. Chen, J. Xu, J. Shuai, J. Chen, Z. Zhang and W. Fang: The S-layer proteins of Lactobacillus crispatus strain ZJ001 is responsible for competitive exclusion against Escherichia coli O157:H7 and Salmonella typhimurium. *Int J Food Microbiol*, 115(3), 307-12 (2007)

59. W. I. Weis, M. E. Taylor and K. Drickamer: The C-type lectin superfamily in the immune system. *Immunol Rev*, 163, 19-34 (1998)

60. M. Murai, O. Turovskaya, G. Kim, R. Madan, C. L. Karp, H. Cheroutre and M. Kronenberg: Interleukin 10 acts on regulatory T cells to maintain expression of the transcription factor Foxp3 and suppressive function in mice with colitis. *Nat Immunol* (2009)

61. M. Rimoldi, M. Chieppa, V. Salucci, F. Avogadri, A. Sonzogni, G. M. Sampietro, A. Nespoli, G. Viale, P. Allavena and M. Rescigno: Intestinal immune homeostasis is regulated by the crosstalk between epithelial cells and dendritic cells. *Nat Immunol*, 6(5), 507-14 (2005)

62. C. S. Wong, S. Jelacic, R. L. Habeeb, S. L. Watkins and P. I. Tarr: The risk of the hemolytic-uremic syndrome after antibiotic treatment of Escherichia coli O157:H7 infections. *N Engl J Med*, 342(26), 1930-6 (2000)

63. N. Safdar, A. Said, R. E. Gangnon and D. G. Maki: Risk of hemolytic uremic syndrome after antibiotic treatment of Escherichia coli O157:H7 enteritis: a meta-analysis. *JAMA*, 288(8), 996-1001 (2002)

64. J. P. Chouraqui, D. Grathwohl, J. M. Labaune, J. M. Hascoet, I. de Montgolfier, M. Leclaire, M. Giarre and P. Steenhout: Assessment of the safety, tolerance, and protective effect against diarrhea of infant formulas containing mixtures of probiotics or probiotics and prebiotics in a randomized controlled trial. *Am J Clin Nutr*, 87(5), 1365-73 (2008)

Abbreviations: MIMP: micro integral membrane protein, TJ tight junction; DCs: dendritic cells, IBD: inflammatory bowel disease, UC: ulcerative colitis, CD: Crohn's disease; SLPs: surface layer proteins; CLR: C-type lectin receptor; IMP: integrated membrane protein; EIEC: enteroinvasive Escherichia coli; E. coli; EPEC: enteropathogenic DC-SIGN: DC-specific ICAM-3-grabbing nonintegrin; TER: transepithelial electrical resistance; PD: potential difference; HPLC: high-performance liquid chromatography

Key Words: Domain; Micro Integral Membrane Protein, Surface Layer Protein, Lactobacillus Plantarum, NCM460, Dendritic Cells, IL-10-/- mice, tight junction

Send correspondence to: Huanlong Qin, Department of Surgery, Shanghai Jiao Tong University Affiliated Sixth People's Hospital, 600 Yishan Road, Shanghai, 200233, China, Tel: 86-21-64369181-8845, Fax: 86-21-64368920, E-mail: hlqin88@126.com